Energy budget and optical theorem for scattering of source-induced fields

Alexander E. Moskalensky and Maxim A. Yurkin*
Voevodsky Institute of Chemical Kinetics and Combustion SB RAS, Institutskaya Street 3, 630090 Novosibirsk, Russia and Novosibirsk State University, Pirogova Street 2, 630090 Novosibirsk, Russia

(Received 19 November 2018; published 16 May 2019)

We provide rigorous definitions of various components of the energy budget for scattering of source-induced electromagnetic fields by a finite nonmagnetic object. We use the classical volume-integral-equation (VIE) framework and define power rates in terms of integrals of the Poynting vector over various surfaces, enclosing some or all of the impressed sources, scatterer, and environment (such as a planar multilayered substrate). Thus, we generalize the conventional cross sections and obtain new interrelations analogous to the well-known optical theorem. We rigorously treat the strong singularity of the VIE kernel, but keep derivations accessible to a wide audience. The defined power rates are further related to the decay rate enhancement and apparent quantum yield of an arbitrary emitter, which are the core concepts in nanophotonics, surface-enhanced Raman scattering, and electron energy-loss spectroscopy. We also discuss the practical calculation of the power rates and decay rate enhancements in the framework of the discrete dipole approximation (DDA). In particular, we derive the volume-integral expression for the scattered power and use it to prove the automatic satisfaction of the optical theorem irrespective of the discretization level. Thus, the optical theorem cannot be used as an internal measure of the DDA accuracy.

DOI: 10.1103/PhysRevA.99.053824

I. INTRODUCTION

Interaction of electromagnetic radiation with particles (commonly referred to as light scattering) forms a basis of many physical phenomena and is ubiquitous in various applications. The frequency-domain volume-integral equation (VIE) is a general framework for theoretical analysis and numerical simulations of scattering by particles of arbitrary shape and internal structure. The VIE has been known for more than 60 years [1] and widely studied during that time [2–4]. However, a number of issues remained, which recently revived the interest in this subject. This led to a rigorous derivation of the VIE for a set of multilayered particles with sharp edges and corners [5], further extended to general incident fields, including those caused by sources located near the scatterer [6,7]. The only missing element is the energy budget for such a general scattering problem. Optical cross sections (extinction, absorption, and scattering) are defined through the power rates (integrals of the Poynting vectors over the closed surfaces) in many textbooks on light-scattering theory [3,8]. However, those definitions are incomplete and/or ambiguous in the case of source-induced fields.

Electromagnetic sources are naturally related to quantum emitters (atoms, molecules, or nanoparticles). While a lot of literature is devoted to corresponding enhancement of emission and decay rates [9–11], it usually considers only local energy balance at the emitter, but neither the flows of the Poynting vector nor the optical cross sections. Quantum electrodynamics (QED) is the rigorous framework describing the emission enhancement [9], but quasiclassical considerations often lead to the same results with intuitive understanding. Fundamentally, those two approaches are connected via the source Green's dyadic, which describes both the local density of states (LDOS) of the quantum system [9] and the classical scattering of radiation and energy transfer [3]. Another quantum process is the surface-enhanced Raman scattering (SERS), where the intensity can be obtained as a combination of classical near-field enhancement of the incident beam (by the scatterer) at one frequency and emission enhancement at a shifted one [12]. Electron energy-loss spectroscopy (EELS) and cathodoluminescence boil down to interaction of the electron-induced field with nanoparticles, but the corresponding quasiclassical descriptions are also typically focused on local energy balance [13,14], with the notable exception of [15]. In summary, the source-induced fields are widely used in many applications, including optimization of microwave antennas, complicated light sources, and fluorescent microscopy. But the corresponding power-flux considerations and simulations, including those with the VIE methods [16], either are local to the emitter or focus on finite-aperture integrals of the far field. Thorough consideration of total scattered power seems to be missing, although it may have only minor direct importance for those applications.

Apart from its fundamental value for theoretical analysis, the VIE forms the basis for a number of "numerically exact" computational methods to simulate electromagnetic scattering, the most popular one being the discrete dipole approximation (DDA) [17]. On one hand, the DDA has been successfully applied to all types of emission enhancement—fluorescence [18,19], SERS [20], and EELS [13,14]. On the other hand, those applications suffer from incomplete understanding of the energy budget described above, complicating their generalizations to complex environments, although see

*Corresponding author: yurkin@gmail.com

[21,22] for the first steps. Moreover, there exists a controversy about the use of the optical theorem to quantify the accuracy of a particular DDA simulation, suggested in [23] but later criticized in [18].

The goal of this paper is threefold. First, we fill the essential gap in the classical VIE framework for general source-induced incident fields, in terms of energy budget among the sources, scatterer, far field, and environment (e.g., a semi-infinite substrate). We rigorously treat the strong singularity of the VIE kernel, but keep derivations as simple and thorough as possible to make the paper accessible to a wide audience. Second, we relate those power rates to the decay rate enhancement of a point emitter, gaining insights into this widely studied phenomenon, especially in the presence of a substrate. Third, we discuss the practical calculation of all power rates in the framework of the DDA and resolve the long-standing controversy related to the optical theorem.

We start by recalling the general VIE framework for the scattering problem in Secs. II and III and give a rigorous definition of the scattered field *inside* the scatterer after the VIE is discretized. Sections IV and V provide the core results of the paper, including definitions of various power rates (flow integrals of the Poynting vector) and interconnections between them. In particular, we derive the volume-integral expression for the scattered power. In Sec. VI we use these power rates to calculate the decay rate enhancement and apparent quantum yield for an emitter with arbitrary intrinsic quantum yield. We also relate those classical results to that based on the quantum perturbation theory. Section VII deals with actual calculation of the power rates in the framework of the DDA. In particular, we derive general conditions under which the optical theorem is exactly satisfied for arbitrary discretization. We consider the limit of distant sources in Sec. VIII, recovering among others the classical result for the plane incident wave. In Sec. IX we generalize the previous results, including decay rate enhancements, to a general environment using a planar substrate (homogeneous half space or multilayered) as an example. Section X concludes the paper.

II. STATEMENT OF THE PROBLEM

The light-scattering problem implies the definition of the incident wave—an electromagnetic wave in a host medium when the scatterer is absent. The classical example is a plane wave, but in this paper we are interested in a broader class of incident fields. Let us follow the formalism presented in [5,6] and define the fields in terms of prescribed current density of external sources $\mathbf{J}_{\rm s}(\mathbf{r})$, oscillating with $\exp(-i\omega t)$ time dependence. In contrast to the free-current density, they are independent of the resulting electromagnetic field. We assume that $\mathbf{J}_{\rm s}(\mathbf{r})$ is sufficiently regular but may include delta functions (point dipoles)—this is further discussed in Sec. III. The incident (or "source-generated") electromagnetic field satisfies the following Maxwell equations in $\mathbb{R}^3$:

$$\begin{aligned}\nabla\times\mathbf{E}_{\rm inc}(\mathbf{r}) &= i\omega\mu_0\mathbf{H}_{\rm inc}(\mathbf{r}),\\ \nabla\times\mathbf{H}_{\rm inc}(\mathbf{r}) &= -i\omega\varepsilon_0\mathbf{E}_{\rm inc}(\mathbf{r})+\mathbf{J}_{\rm s}(\mathbf{r}).\end{aligned}\tag{1}$$

For simplicity, we assume that the host medium is nonmagnetic and has the dielectric permittivity of the vacuum, but all derivations can be trivially extended to any positive real permittivity.

The scatterer is a nonmagnetic object with finite volume $V_{\rm int}$ and complex refractive index $m(\mathbf{r})$. The presence of the object changes the total electromagnetic field everywhere in the space, including $V_{\rm int}$ and the external volume $V_{\rm ext}=\mathbb{R}^3\backslash V_{\rm int}$. This field satisfies the following Maxwell equations:

$$\begin{aligned}\nabla\times\mathbf{E}(\mathbf{r}) &= i\omega\mu_0\mathbf{H}(\mathbf{r}),\\ \nabla\times\mathbf{H}(\mathbf{r}) &= -i\omega\varepsilon(\mathbf{r})\mathbf{E}(\mathbf{r})+\mathbf{J}_{\rm s}(\mathbf{r}),\end{aligned}\tag{2}$$

where $\varepsilon(\mathbf{r})$ is the dielectric permittivity in the whole space, defined as

$$\varepsilon(\mathbf{r}) \stackrel{\rm def}{=} \begin{cases}\varepsilon_0, & \mathbf{r}\in V_{\rm ext},\\ \varepsilon_0 m^2(\mathbf{r}), & \mathbf{r}\in V_{\rm int}.\end{cases}\tag{3}$$

According to Eq. (2), external sources may be present both inside and outside the object; however, in the majority of applications sources are located outside the scatterer. Below, we assume that the volume occupied by the sources $V_{\rm s}$ is a finite subvolume of $V_{\rm ext}$. The scattered field is defined as the total field *minus* the incident field:

$$\begin{aligned}\mathbf{E}_{\rm sca}(\mathbf{r}) &\stackrel{\rm def}{=} \mathbf{E}(\mathbf{r})-\mathbf{E}_{\rm inc}(\mathbf{r}),\\ \mathbf{H}_{\rm sca}(\mathbf{r}) &\stackrel{\rm def}{=} \mathbf{H}(\mathbf{r})-\mathbf{H}_{\rm inc}(\mathbf{r}).\end{aligned}\tag{4}$$

III. GENERAL VOLUME-INTEGRAL-EQUATION FRAMEWORK

The solution of the light-scattering problem should satisfy Eq. (2) together with boundary conditions on the surface of the object (potentially nonsmooth) and at infinity. One way to find the electric field which meets these requirements is through the equivalent VIE [5], also known as the Lippmann-Schwinger equation:

$$\begin{aligned}\mathbf{E}(\mathbf{r}) = \mathbf{E}_{\rm inc}(\mathbf{r})+k^2\lim_{V_0\to 0}\int_{\mathbb{R}^3\backslash V_0} d^3\mathbf{r}'[m^2(\mathbf{r}')-1]\bar{\mathbf{G}}(\mathbf{r},\mathbf{r}')\cdot\mathbf{E}(\mathbf{r}')\\ -\frac{m^2(\mathbf{r})-1}{3}\mathbf{E}(\mathbf{r}),\end{aligned}\tag{5}$$

where V_0 is the spherical exclusion volume centered at $\mathbf{r}$ [24], k is the wave number in a host medium (λ is the corresponding wavelength), and $\bar{\mathbf{G}}(\mathbf{r},\mathbf{r}')$ is the free-space dyadic Green's function, defined as

$$\begin{aligned}\bar{\mathbf{G}}(\mathbf{r},\mathbf{r}')=\bar{\mathbf{G}}(\mathbf{R})=\left(\bar{\mathbf{I}}+\frac{\nabla\otimes\nabla}{k^2}\right)\frac{\exp(ikR)}{4\pi R}=\frac{\exp(ikR)}{4\pi R}\\ \times\left[\left(\bar{\mathbf{I}}-\frac{\mathbf{R}\otimes\mathbf{R}}{R^2}\right)+\frac{ikR-1}{k^2R^2}\left(\bar{\mathbf{I}}-3\frac{\mathbf{R}\otimes\mathbf{R}}{R^2}\right)\right],\end{aligned}\tag{6}$$

where $\mathbf{R}=\mathbf{r}-\mathbf{r}'$, $R=|\mathbf{R}|$, and $\mathbf{R}\otimes\mathbf{R}$ is a dyadic: $(\mathbf{R}\otimes\mathbf{R})_{\mu\nu}=\mathbf{R}_\mu\mathbf{R}_\nu$ (μ and ν are Cartesian components of the vector or dyadic). The exclusion of V_0 is needed to avoid the singularity of the Green's dyadic ($\sim R^{-3}$); the integral of this singular part over V_0 is replaced by a surface integral. It gives the last term in (5), the so-called L term or self-term, which

is regular and does not depend on the size of V_0. In contrast, the integral of the rest of the Green's dyadic scales together with $V_0(\mathbf{r})$, and is nonzero in computations (the so-called M term)—see Eq. (12) below.

While the free-space case is the most common in applications (and an infinite homogeneous medium is equivalent to it), other environments are also relevant, such as the semi-infinite plane substrate (Sec. IX). Then the whole theoretical framework remains valid, but $\bar{\mathbf{G}}$ should be replaced by that corresponding to a particular environment. Thus, we further perform all derivations for arbitrary $\bar{\mathbf{G}}$ and note explicitly when Eq. (6) is used to obtain the free-space result.

Some authors express the VIE in terms of forcing function $\mathbf{j}(\mathbf{r}) \stackrel{\text{def}}{=} k^2[m^2(\mathbf{r})-1]\mathbf{E}(\mathbf{r})$ or the polarization density $\mathbf{P}(\mathbf{r}) \stackrel{\text{def}}{=} [\varepsilon(\mathbf{r})-\varepsilon_0]\mathbf{E}(\mathbf{r})$. The latter leads to the following VIE representation,

$$\frac{1}{3\varepsilon_0}\frac{\varepsilon(\mathbf{r})+2\varepsilon_0}{\varepsilon(\mathbf{r})-\varepsilon_0}\mathbf{P}(\mathbf{r}) = \mathbf{E}_{\text{inc}}(\mathbf{r}) + \omega^2\mu_0 \lim_{V_0\to 0}\int_{\mathbb{R}^3\setminus V_0} d^3\mathbf{r}'\bar{\mathbf{G}}(\mathbf{r},\mathbf{r}')\cdot\mathbf{P}(\mathbf{r}'), \quad (7)$$

and the expression for the scattered field:

$$\mathbf{E}_{\text{sca}}(\mathbf{r}) = \omega^2\mu_0 \lim_{V_0\to 0}\int_{\mathbb{R}^3\setminus V_0} d^3\mathbf{r}'\bar{\mathbf{G}}(\mathbf{r},\mathbf{r}')\cdot\mathbf{P}(\mathbf{r}') - \frac{\mathbf{P}(\mathbf{r})}{3\varepsilon_0}, \quad (8)$$

which is valid both outside and inside the object. Equations (7) and (8) are trivial consequences of the classical Eq. (5), but they have not been explicitly considered before.

Importantly, the VIE holds true in the presence of sources, even if they are inside the object [6]. Then $\mathbf{E}_{\text{inc}}$ in (5) is expressed as a similar volume integral:

$$\mathbf{E}_{\text{inc}}(\mathbf{r}) = i\omega\mu_0 \lim_{V_0\to 0}\int_{V_s\setminus V_0} d^3\mathbf{r}'\bar{\mathbf{G}}(\mathbf{r},\mathbf{r}')\cdot\mathbf{J}_s(\mathbf{r}') - i\frac{\mathbf{J}_s(\mathbf{r})}{3\omega\varepsilon_0}, \quad (9)$$

where the explicit exclusion of the singularity makes it valid in the whole $\mathbb{R}^3$. The regularity of $\mathbf{E}_{\text{inc}}$ is fully determined by $\mathbf{J}_s$. The simplest case is that of a square-integrable (finite-energy) $\mathbf{J}_s$ in a finite V_s, resulting in square-integrable $\mathbf{E}_{\text{inc}}$. A convenient abstraction is a point dipole, given by $\mathbf{J}_s(\mathbf{r}) = \mathbf{J}_0\delta(\mathbf{r}-\mathbf{r}_0)$, or a combination of several such dipoles. Then $\mathbf{J}_s$ is square integrable almost everywhere and so is $\mathbf{E}_{\text{inc}}$. The latter is fine for most derivations except when we apply the divergence theorem for the surface enclosing the singularity. One option would be to consider a point dipole (delta function) as a limit of physically realistic dipoles of a finite size. But to avoid potential ambiguities we will further explicitly exclude the singularities in the corresponding integrals; then the details of the physical realization of the delta function are not relevant. Another abstraction is that of the infinitely distant sources (discussed in Sec. VIII)—the resulting $\mathbf{E}_{\text{inc}}$ has no singularities near the particle, but is only locally square integrable, i.e., in any finite volume. We will denote the latter case further as the "source-free" one, although this definition is not completely rigorous.

Most implementations of the DDA are based on solving Eq. (7) given any specific $\mathbf{E}_{\text{inc}}$ [25]. The first step is to represent an object as a set of voxels with centers at $\mathbf{r}_i$ (dipoles), which are small enough to consider all the relevant functions constant inside the voxel (refractive index, fields, Green's dyadic from another voxel, etc.). Here and below, index i is used for dipoles and sources. It is used only in subscripts and summation indexes not to be confused with imaginary unit. The voxels may have different shapes and volumes [26], but we consider only the simplest case of a cubical grid with edge size d. Inside each voxel we can evaluate Eq. (7) at $\mathbf{r}=\mathbf{r}_i$ and approximate the integral with a sum over all N dipoles, leading to

$$\bar{\boldsymbol{\alpha}}_i^{-1}\cdot\mathbf{P}_i = \mathbf{E}_{\text{inc},i} + \omega^2\mu_0\sum_{j\neq i}\bar{\mathbf{G}}_{ij}\cdot\mathbf{P}_j, \quad (10)$$

where $\mathbf{E}_{\text{inc},\,i} \stackrel{\text{def}}{=} \mathbf{E}_{\text{inc}}(\mathbf{r}_i)$, $\bar{\mathbf{G}}_{ij} \stackrel{\text{def}}{=} \bar{\mathbf{G}}(\mathbf{r}_i,\mathbf{r}_j)$ (in the simplest DDA formulation that we consider here), $\mathbf{P}_i \stackrel{\text{def}}{=} \mathbf{P}(\mathbf{r}_i)V_{\text{d}}$ is the total polarization of the dipole (note the scaling factor of dipole volume V_{d}), and $\bar{\boldsymbol{\alpha}}_i$ is the dipole polarizability dyadic [26]:

$$\bar{\boldsymbol{\alpha}}_i = \varepsilon_0 V_{\text{d}}\left(\frac{1}{3}\frac{\varepsilon_i+2\varepsilon_0}{\varepsilon_i-\varepsilon_0}\bar{\mathbf{I}} - \bar{\mathbf{M}}_i\right)^{-1}, \quad (11)$$

where $\varepsilon_i \stackrel{\text{def}}{=} \varepsilon(\mathbf{r}_i)$ and $\bar{\mathbf{M}}_i$ approximates the self-integral with excluded singularity:

$$k^2 \lim_{V_0\to 0}\int_{V_i\setminus V_0} d^3\mathbf{r}'\bar{\mathbf{G}}(\mathbf{r},\mathbf{r}')\cdot\mathbf{P}(\mathbf{r}') \approx \bar{\mathbf{M}}_i\cdot\mathbf{P}(\mathbf{r}_i). \quad (12)$$

Here and below, approximation "$\approx$" corresponds to the discretization. The expression for $\bar{\mathbf{M}}_i$ depends on a specific DDA formulation, but its value always decreases with d at least as $\mathcal{O}(d^2)$, since the essential singularity was separated [17].

Equation (10) is typically solved for the unknown polarizations $\mathbf{P}_i$ via an iterative method. As soon as the polarizations are known, one can compute a variety of quantities, for instance, the scattered field outside the object [see Eq. (8)]:

$$\mathbf{E}_{\text{sca}}(\mathbf{r}) \approx \omega^2\mu_0\sum_i \bar{\mathbf{G}}(\mathbf{r},\mathbf{r}_i)\cdot\mathbf{P}_i,\ \ \mathbf{r}\in V_{\text{ext}}. \quad (13)$$

The DDA is a numerically rigorous method, which means that any computed quantity, e.g., $\mathbf{E}_{\text{sca}}(\mathbf{r})$, converges to the true one with refining discretization (as $d\to 0$ and $N\to\infty$) [17]. At the same time the mathematical formulation, in particular, Eqs. (10) and (13), is equivalent to that of the simple phenomenological picture of interacting point dipoles with given polarizabilities (for any $\bar{\mathbf{M}}_i$).

However, the underlying discretization needs to be accounted for when calculating $\mathbf{E}_{\text{sca}}(\mathbf{r})$ inside the particle [or $\mathbf{E}(\mathbf{r})$, see Eq. (4)]. Since we assumed the fields constant over the dipole volume in the beginning, Eq. (8) may be directly used only for $\mathbf{r}=\mathbf{r}_i$ (otherwise the integral over $V_i\setminus V_0$ cannot be neglected), leading to

$$\mathbf{E}_{\text{sca},i} \stackrel{\text{def}}{=} \mathbf{E}_{\text{sca}}(\mathbf{r}_i) \approx \omega^2\mu_0\sum_{j\neq i}\bar{\mathbf{G}}_{ij}\cdot\mathbf{P}_j + \left(\bar{\mathbf{M}}_i - \frac{\bar{\mathbf{I}}}{3}\right)\cdot\frac{\mathbf{P}_i}{V_{\text{d}}\varepsilon_0}. \quad (14)$$

The fields $\mathbf{E}_{\text{sca}}(\mathbf{r})$ between dipole centers should be obtained by interpolation (e.g., nearest-neighbor) of $\mathbf{E}_{\text{sca},i}$. By contrast, incorrectly replacing $\mathbf{r}_i$ by $\mathbf{r}$ in Eq. (14) would lead to dipole-scale variation of the fields, which has nothing to do with

relatively smooth fields inside a homogeneous scatterer. Note also that Eq. (4) implies $\mathbf{E}_{\mathrm{sca},i} = \mathbf{E}_i - \mathbf{E}_{\mathrm{inc},i}$, where $\mathbf{E}_i \overset{\mathrm{def}}{=} \mathbf{E}(\mathbf{r}_i) = \mathbf{P}_i/[V_{\mathrm{d}}(\varepsilon_i - \varepsilon_0)]$.

IV. POWER EMITTED BY SOURCES

Consideration of energy flow in a classical light-scattering problem results in important relations such as the optical theorem [27,28]. The analysis is even more interesting in the case of external sources. Let us briefly recall the derivation in the classical case and extend it to the fields with sources.

The time-averaged rate of electromagnetic energy flow per unit area is given by the Poynting vector [3]:

$$\mathbf{S}(\mathbf{r}) = \frac{1}{2}\mathrm{Re}[\mathbf{E}(\mathbf{r}) \times \mathbf{H}^*(\mathbf{r})]. \tag{15}$$

Here and below, Re and Im denote the real and imaginary part, respectively. Integrating $\mathbf{S}(\mathbf{r})$ over the closed surface A results in the power generated or lost in the volume inside the surface (according to the Poynting theorem):

$$W = \oint_A d\mathbf{A} \cdot \mathbf{S}(\mathbf{r}), \tag{16}$$

where $d\mathbf{A} \overset{\mathrm{def}}{=} \mathbf{n}\, d^2\mathbf{r}$, $\mathbf{n}$ designates the normal to the surface, and the sign is chosen such that W is positive when energy goes outside the surface. Using the divergence theorem, we can transform the surface integral in Eq. (16) into the volume integral of $\nabla\mathbf{S}$, which equals

$$\begin{aligned}
\nabla\mathbf{S}(\mathbf{r}) &= \frac{1}{2}\mathrm{Re}(\nabla \cdot [\mathbf{E}(\mathbf{r}) \times \mathbf{H}^*(\mathbf{r})]) \\
&= \frac{1}{2}\mathrm{Re}([\nabla \times \mathbf{E}(\mathbf{r})] \cdot \mathbf{H}^*(\mathbf{r}) - \mathbf{E}(\mathbf{r}) \cdot [\nabla \times \mathbf{H}^*(\mathbf{r})]) \\
&= \frac{1}{2}\mathrm{Re}[i\omega\mu_0|\mathbf{H}(\mathbf{r})|^2 - i\omega\varepsilon^*(\mathbf{r})|\mathbf{E}(\mathbf{r})|^2 - \mathbf{E}(\mathbf{r}) \cdot \mathbf{J}_{\mathrm{s}}^*(\mathbf{r})] \\
&= -\frac{\omega}{2}|\mathbf{E}(\mathbf{r})|^2\mathrm{Im}[\varepsilon(\mathbf{r})] - \frac{1}{2}\mathrm{Re}[\mathbf{E}(\mathbf{r}) \cdot \mathbf{J}_{\mathrm{s}}^*(\mathbf{r})],
\end{aligned} \tag{17}$$

where we used Eq. (2) for curls. Combining Eqs. (15) and (16) we obtain

$$\begin{aligned}
W = &-\frac{\omega}{2}\int_{V_A} d^3\mathbf{r}|\mathbf{E}(\mathbf{r})|^2\mathrm{Im}[\varepsilon(\mathbf{r})] \\
&-\frac{1}{2}\int_{V_A} d^3\mathbf{r}\ \mathrm{Re}[\mathbf{E}(\mathbf{r}) \cdot \mathbf{J}_{\mathrm{s}}^*(\mathbf{r})],
\end{aligned} \tag{18}$$

where V_A is the volume bounded by the surface A, and we assume that fields and currents are regular inside both V_A and A.

In this section we consider the case when only the sources are present and not the scatterer. If additionally the sources are regular, we substitute Eq. (9) into Eq. (18) to obtain

$$\begin{aligned}
W_0 &= -\frac{1}{2}\int_{V_{\mathrm{s}}} d^3\mathbf{r}\ \mathrm{Re}[\mathbf{E}_{\mathrm{inc}}(\mathbf{r}) \cdot \mathbf{J}_{\mathrm{s}}^*(\mathbf{r})] \\
&= \frac{\omega\mu_0}{2}\int_{V_{\mathrm{s}}} d^3\mathbf{r} \lim_{V_0(\mathbf{r})\to 0}\int_{V_{\mathrm{s}}\setminus V_0(\mathbf{r})} d^3\mathbf{r}' \\
&\quad \times \mathrm{Im}[\mathbf{J}_{\mathrm{s}}^*(\mathbf{r}) \cdot \bar{\mathbf{G}}(\mathbf{r}, \mathbf{r}') \cdot \mathbf{J}_{\mathrm{s}}(\mathbf{r}')],
\end{aligned} \tag{19}$$

where we explicitly specified the exclusion volume center. By definition,

$$\begin{aligned}
&\mathrm{Im}[\mathbf{J}_{\mathrm{s}}^*(\mathbf{r}) \cdot \bar{\mathbf{G}}(\mathbf{r}, \mathbf{r}') \cdot \mathbf{J}_{\mathrm{s}}(\mathbf{r}')] \\
&\quad = \frac{1}{2i}[\mathbf{J}_{\mathrm{s}}^*(\mathbf{r}) \cdot \bar{\mathbf{G}}(\mathbf{r}, \mathbf{r}') \cdot \mathbf{J}_{\mathrm{s}}(\mathbf{r}') - \mathbf{J}_{\mathrm{s}}^*(\mathbf{r}') \cdot \bar{\mathbf{G}}^H(\mathbf{r}, \mathbf{r}') \cdot \mathbf{J}_{\mathrm{s}}(\mathbf{r})],
\end{aligned} \tag{20}$$

where H denotes the Hermitian (conjugate) transpose of a dyadic (matrix) and we used the property of the dyadic transpose: $\mathbf{a} \cdot \bar{\mathbf{G}} \cdot \mathbf{b} = \mathbf{b} \cdot \bar{\mathbf{G}}^T \cdot \mathbf{a}$, $\forall \mathbf{a}, \mathbf{b}$. Note also that the integration volume in the double integral of Eq. (19) is symmetric even accounting for excluded V_0; hence, $\mathbf{r}$ and $\mathbf{r}'$ may be interchanged in the integrand. Doing this interchange in the last term in the right-hand side of Eq. (20), we obtain

$$W_0 = \frac{\omega\mu_0}{2}\iint_{V_{\mathrm{s}}} d^3\mathbf{r}\, d^3\mathbf{r}'\, \mathbf{J}_{\mathrm{s}}^*(\mathbf{r}) \cdot \bar{\mathbf{G}}^I(\mathbf{r}, \mathbf{r}') \cdot \mathbf{J}_{\mathrm{s}}(\mathbf{r}'), \tag{21}$$

where we introduced

$$\bar{\mathbf{G}}^I(\mathbf{r}, \mathbf{r}') \overset{\mathrm{def}}{=} \frac{1}{2i}[\bar{\mathbf{G}}(\mathbf{r}, \mathbf{r}') - \bar{\mathbf{G}}^H(\mathbf{r}', \mathbf{r})], \tag{22}$$

and omitted the exclusion volume because (22) has no singularity for $\mathbf{r} = \mathbf{r}'$, i.e., $\bar{\mathbf{G}}^I(\mathbf{r}, \mathbf{r}) \overset{\mathrm{def}}{=} \lim_{\mathbf{r}'\to\mathbf{r}} \bar{\mathbf{G}}^I(\mathbf{r}, \mathbf{r}')$ is finite [as far as the host medium is nonabsorbing [29]; see Eq. (25) for a free space]. $\bar{\mathbf{G}}^I(\mathbf{r}, \mathbf{r}')$ is a symmetric (self-adjoint) operator kernel [30], i.e., $\bar{\mathbf{G}}^I(\mathbf{r}, \mathbf{r}') = [\bar{\mathbf{G}}^I(\mathbf{r}', \mathbf{r})]^H$, guaranteeing that the integral in Eq. (21) is always real. A similar kernel has recently been used for radiative heat transfer in a nonreciprocal environment [31]. By contrast, $\bar{\mathbf{G}}^I(\mathbf{r}, \mathbf{r}') = \mathrm{Im}[\bar{\mathbf{G}}(\mathbf{r}, \mathbf{r}')]$ in any reciprocal environment, i.e., when $\bar{\mathbf{G}}(\mathbf{r}, \mathbf{r}') = \bar{\mathbf{G}}^T(\mathbf{r}', \mathbf{r})$ [6,32].

Equation (21) is valid for any integrable distribution of currents, which can be derived by a continuous transformation of regular ones. Moreover, $\bar{\mathbf{G}}^I(\mathbf{r}, \mathbf{r}')$ may be replaced by a constant for sufficiently small V_{s}, i.e., when all linear dimensions of V_{s} are much smaller than both λ and characteristic geometric scales of the environment. We will further refer to these conditions as the "static limit" although, strictly speaking, this name is more appropriate for the long-wavelength limit alone. The second condition (e.g., the relation to the distance from V_{s} to the plane substrate, as discussed in Sec. IX) can be more restrictive. In this static limit (denoted as $V_{\mathrm{s}} \to 0$), one obtains

$$\lim_{V_{\mathrm{s}}\to 0} W_0 = \frac{\omega\mu_0}{2}\mathbf{J}_0^* \cdot \bar{\mathbf{G}}^I(\mathbf{u}_0, \mathbf{u}_0) \cdot \mathbf{J}_0, \tag{23}$$

where $\mathbf{J}_0$ is the total current,

$$\mathbf{J}_0 \overset{\mathrm{def}}{=} \int_{V_{\mathrm{s}}} d^3\mathbf{r}\, \mathbf{J}_{\mathrm{s}}(\mathbf{r}), \tag{24}$$

and $\mathbf{u}_0$ is any point inside V_{s}. In other words, the retardation may be neglected. However, that does not mean that the Green's dyadic is purely real—that would imply a zero value of Eq. (19); rather its small but significant imaginary part has to be properly separated.

In the free space, Eq. (6) implies [see Eq. (A7) in the Appendix]

$$\bar{\mathbf{G}}^I(\mathbf{r},\mathbf{r}) = \lim_{\mathbf{r}'\to\mathbf{r}} \mathrm{Im}[\bar{\mathbf{G}}(\mathbf{r},\mathbf{r}')] = \frac{k\bar{\mathbf{I}}}{6\pi}, \tag{25}$$

leading to the classical result for the power emitted by a point dipole with dipole moment $i\mathbf{J}_0/\omega$, e.g., [4,9]. However, it is instructive to derive the same result explicitly for $\mathbf{J}_s(\mathbf{r}) = \mathbf{J}_0\delta(\mathbf{r}-\mathbf{u}_0)$. We take A to be a sphere (of radius R) centered at $\mathbf{u}_0$:

$$\begin{aligned} W_0 &= \oint_A d\mathbf{A}\cdot\mathbf{S}(\mathbf{r}) = \frac{1}{2}\oint_A d^2\mathbf{r}\,\mathrm{Re}\{(\mathbf{n}\times\mathbf{E}_{\mathrm{inc}}(\mathbf{r}))\cdot\mathbf{H}_{\mathrm{inc}}(\mathbf{r})^*\} \\ &= -\frac{\omega\mu_0}{2}\oint_A d^2\mathbf{r}\,\mathrm{Im}\{[(\mathbf{n}\times\bar{\mathbf{G}}(\mathbf{r},\mathbf{u}_0))\cdot\mathbf{J}_0]\cdot[(\nabla\times\bar{\mathbf{G}}(\mathbf{r},\mathbf{u}_0))\cdot\mathbf{J}_0]^*\} \\ &= -\frac{\omega\mu_0}{2}\oint_A d^2\mathbf{r}\,\mathrm{Im}\left\{(\mathbf{n}\times\mathbf{J}_0)\frac{\exp(ikR)}{4\pi R}\left(1+\frac{ikR-1}{k^2R^2}\right)\cdot\left[(\mathbf{n}\times\mathbf{J}_0)\frac{\exp(ikR)}{4\pi R^2}(ikR-1)\right]^*\right\} \\ &= \frac{\omega\mu_0 k}{8\pi}\frac{1}{4\pi R^2}\oint_A d^2\mathbf{r}\,\mathbf{J}_0\cdot(\bar{\mathbf{I}}-\mathbf{n}\otimes\mathbf{n})\cdot\mathbf{J}_0^* = \frac{\omega^2\mu_0}{12\pi c}|\mathbf{J}_0|^2, \end{aligned} \tag{26}$$

where we used Eqs. (6) and (15) and the fact that averaging $\mathbf{n}\otimes\mathbf{n}$ over all directions results in $\bar{\mathbf{I}}/3$.

To conclude this section, we consider a rather general case of regular source distribution $\mathbf{J}_r(\mathbf{r})$ combined with a finite number of simple singularities, i.e.,

$$\mathbf{J}_s(\mathbf{r}) = \mathbf{J}_r(\mathbf{r}) + \sum_i \mathbf{J}_i\delta(\mathbf{r}-\mathbf{u}_i). \tag{27}$$

Then the answer is given by Eq. (21), but it can be expanded as

$$\begin{aligned} W_0 = \frac{\omega\mu_0}{2}\Bigg\{ &\iint_{V_s} d^3\mathbf{r}\,d^3\mathbf{r}'\,\mathbf{J}_r^*(\mathbf{r})\cdot\bar{\mathbf{G}}^I(\mathbf{r},\mathbf{r}')\cdot\mathbf{J}_r(\mathbf{r}') \\ &+2\sum_i\int_{V_s} d^3\mathbf{r}\,\mathbf{J}_i^*\cdot\bar{\mathbf{G}}^I(\mathbf{u}_i,\mathbf{r})\cdot\mathbf{J}_r(\mathbf{r}) \\ &+\sum_{i,j}\mathbf{J}_i^*\cdot\bar{\mathbf{G}}^I(\mathbf{u}_i,\mathbf{u}_j)\cdot\mathbf{J}_j\Bigg\}. \end{aligned} \tag{28}$$

If there are only point dipoles, then only the double sum remains in Eq. (28).

V. ENERGY BUDGET FOR SOURCES NEAR A SCATTERER

Let us add the scattering object to our consideration. Then the physical meaning of Eq. (16) depends on the surface of integration. We further define three different surfaces (Fig. 1): A_1 covers the object and not the sources, A_2 covers the sources and not the object, and A_3 covers both the object and the sources.

Since there are no sources inside A_1 and $\mathrm{Im}[\varepsilon(\mathbf{r})] = 0$ outside the object, the integration of Eq. (17) over A_1 yields the conventional absorption power:

$$W_{\mathrm{abs}} \overset{\mathrm{def}}{=} -\oint_{A_1} d\mathbf{A}\cdot\mathbf{S}(\mathbf{r}) = \frac{\omega}{2}\int_{V_{\mathrm{int}}} d^3\mathbf{r}\,|\mathbf{E}(\mathbf{r})|^2\mathrm{Im}[\varepsilon(\mathbf{r})]. \tag{29}$$

Note the opposite sign as compared to Eq. (17) since W_{abs} is the power which goes inside the volume. The integration around the sources yields the emission power [33]:

$$W_{\mathrm{em}} \overset{\mathrm{def}}{=} \oint_{A_2} d\mathbf{A}\cdot\mathbf{S}(\mathbf{r}) = -\frac{1}{2}\int_{V_S} d^3\mathbf{r}\,\mathrm{Re}[\mathbf{E}(\mathbf{r})\cdot\mathbf{J}_s^*(\mathbf{r})], \tag{30}$$

where the singularities, if present, should be treated analogously to Eqs. (26) and (28). Finally, the integration around both the sources and the object represents the total rate of energy radiation from the system:

$$W_{\mathrm{rad}} \overset{\mathrm{def}}{=} \oint_{A_3} d\mathbf{A}\cdot\mathbf{S}(\mathbf{r}) = W_{\mathrm{em}} - W_{\mathrm{abs}}. \tag{31}$$

It is important to note that the surfaces may be arbitrarily deformed as long as they intersect neither the sources nor the object. For instance, it is sometimes more convenient to integrate fields in a far zone ($A_3 \to$ large sphere). A_1 and A_2 may be shrunk to the boundaries of the object and the sources, respectively. Moreover, as the normal component of the Poynting vector is continuous when passing through the boundary of the object (in contrast to the fields), A_1 may also be considered on the internal side of the object boundary.

It is common to define scattering and extinction power rates by separating the Poynting vector into three components [3]. This approach can be used for source-induced fields without any changes:

$$\mathbf{S} = \mathbf{S}_{\mathrm{inc}} + \mathbf{S}_{\mathrm{sca}} + \mathbf{S}_{\mathrm{ext}},\ \mathbf{S}_{\mathrm{inc}} \overset{\mathrm{def}}{=} \frac{1}{2}\mathrm{Re}(\mathbf{E}_{\mathrm{inc}}\times\mathbf{H}_{\mathrm{inc}}^*),$$

$$\mathbf{S}_{\mathrm{sca}} \overset{\mathrm{def}}{=} \frac{1}{2}\mathrm{Re}(\mathbf{E}_{\mathrm{sca}}\times\mathbf{H}_{\mathrm{sca}}^*),$$

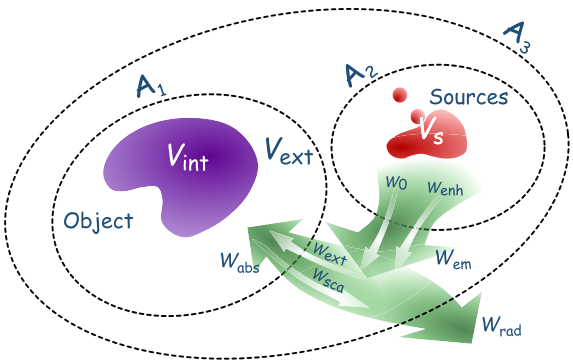

FIG. 1. Definitions of geometry and energy flows, when the sources are located near the scattering object. All symbols are defined in the text.

$$\mathbf{S}_{\rm ext} \stackrel{\rm def}{=} \frac{1}{2}{\rm Re}(\mathbf{E}_{\rm inc}\times\mathbf{H}^*_{\rm sca}+\mathbf{E}_{\rm sca}\times\mathbf{H}^*_{\rm inc}). \tag{32}$$

Using Eqs. (1)–(4), we obtain the divergence of each component [see Eq. (17)]:

$$\begin{aligned}\nabla\mathbf{S}_{\rm inc} &= -\frac{1}{2}{\rm Re}(\mathbf{E}_{\rm inc}\cdot\mathbf{J}^*_{\rm s}),\\ \nabla\mathbf{S}_{\rm sca} &= \frac{\omega}{2}{\rm Im}[\mathbf{E}_{\rm sca}\cdot(\varepsilon^*(\mathbf{r})-\varepsilon_0)\mathbf{E}^*] = \frac{\omega}{2}{\rm Im}(\mathbf{E}_{\rm sca}\cdot\mathbf{P}^*),\\ \nabla\mathbf{S}_{\rm ext} &= \frac{\omega}{2}{\rm Im}[\mathbf{E}_{\rm inc}\cdot\mathbf{P}^*]-\frac{1}{2}{\rm Re}(\mathbf{E}_{\rm sca}\cdot\mathbf{J}^*_{\rm s}).\end{aligned} \tag{33}$$

Let us first consider the energy balance inside the object. Integrating $\nabla\mathbf{S}_{\rm sca}$ over A_1, as in the source-free case, results in the scattered power:

$$W_{\rm sca} \stackrel{\rm def}{=} \oint_{A_1} d\mathbf{A}\cdot\mathbf{S}_{\rm sca}(\mathbf{r}) = \frac{\omega}{2}\int_{V_{\rm int}} d^3\mathbf{r}\ {\rm Im}[\mathbf{E}_{\rm sca}(\mathbf{r})\cdot\mathbf{P}^*(\mathbf{r})]. \tag{34}$$

According to Eq. (8), this equals

$$\begin{aligned}W_{\rm sca} &= \frac{\omega^3\mu_0}{2}\int_{V_{\rm int}} d^3\mathbf{r}\\ &\quad\times{\rm Im}\left[\mathbf{P}^*(\mathbf{r})\cdot\lim_{V_0(\mathbf{r})\to 0}\int_{V_{\rm int}\setminus V_0(\mathbf{r})} d^3\mathbf{r}'\bar{G}(\mathbf{r},\mathbf{r}')\cdot\mathbf{P}(\mathbf{r}')\right]\\ &= \frac{\omega^3\mu_0}{2}\iint_{V_{\rm int}} d^3\mathbf{r}d^3\mathbf{r}'\,\mathbf{P}^*(\mathbf{r})\cdot\bar{\mathbf{G}}^I(\mathbf{r},\mathbf{r}')\cdot\mathbf{P}(\mathbf{r}'),\end{aligned} \tag{35}$$

where the last transformation is analogous to that from Eq. (19) to Eq. (21). The volume-integral representation of the scattered power is rarely found in the literature, with only a few exceptions [34–36] that do not explicitly discuss the singularity. This representation is convenient for computations, especially in the DDA, as discussed in Sec. VII. Moreover, it was recently used to rigorously prove the additivity of scattering cross sections for a fixed multiparticle group under the single-scattering approximation [37].

The conventional approach to obtain the scattering power is the integration over a sphere in the far zone, at least in the free space. In this case Eq. (8) implies

$$\mathbf{E}_{\rm sca}(\mathbf{r}) \underset{r\to\infty}{\to} \frac{\exp(ikr)}{r}\mathbf{F}\left(\frac{\mathbf{r}}{r}\right), \tag{36}$$

which defines the far-field scattering amplitude $\mathbf{F}$ ($\mathbf{n}$ is a unit vector):

$$\mathbf{F}(\mathbf{n}) = \frac{\omega^2\mu_0}{4\pi}(\bar{\mathbf{I}}-\mathbf{n}\otimes\mathbf{n})\cdot\int_{V_{\rm int}} d^3\mathbf{r}'\exp(-ik\mathbf{r}'\cdot\mathbf{n})\mathbf{P}(\mathbf{r}'). \tag{37}$$

Choosing A_3 to be a very large sphere we transform the integral to that over a unit sphere:

$$W_{\rm sca} = \frac{k}{2\omega\mu_0}\oint d^2\mathbf{n}\ |\mathbf{F}(\mathbf{n})|^2. \tag{38}$$

While Eq. (38) seems to be very different from Eq. (35), their equivalence can be proven directly by substituting Eq. (37) into Eq. (38), changing the integration order, and using the algebraic identity

$$\bar{\mathbf{G}}^I(\mathbf{r},\mathbf{r}') = \frac{k}{(4\pi)^2}\oint d^2\mathbf{n}\exp[ik(\mathbf{r}-\mathbf{r}')\cdot\mathbf{n}](\bar{\mathbf{I}}-\mathbf{n}\otimes\mathbf{n}), \tag{39}$$

which is derived in the Appendix [see Eq. (A6)]. It is also natural to introduce the far-field amplitude $\mathbf{F}_{\rm inc}$ of the source-generated incident field by replacing $\mathbf{E}_{\rm sca}$, $\mathbf{F}$, $\mathbf{P}$, $V_{\rm int}$, and $W_{\rm sca}$ in Eqs. (36)–(38) by $\mathbf{E}_{\rm inc}$, $\mathbf{F}_{\rm inc}$, $i\mathbf{J}_{\rm s}/\omega$, $V_{\rm s}$, and W_0, respectively, i.e.,

$$\mathbf{F}_{\rm inc}(\mathbf{n}) = \frac{i\omega\mu_0}{4\pi}(\bar{\mathbf{I}}-\mathbf{n}\otimes\mathbf{n})\cdot\int_{V_{\rm s}} d^3\mathbf{r}'\exp(-ik\mathbf{r}'\cdot\mathbf{n})\mathbf{J}_{\rm s}(\mathbf{r}'), \tag{40}$$

$$W_0 = \frac{k}{2\omega\mu_0}\oint d^2\mathbf{n}\ |\mathbf{F}_{\rm inc}(\mathbf{n})|^2. \tag{41}$$

A small-particle (static) limit can be obtained from Eq. (35) analogously to Eq. (23):

$$\lim_{V_{\rm int}\to 0} W_{\rm sca} = \frac{\omega^3\mu_0}{2}\mathbf{P}^*_\Sigma\cdot\bar{\mathbf{G}}^I(\mathbf{r},\mathbf{r})\cdot\mathbf{P}_\Sigma, \tag{42}$$

where $\mathbf{r}\in V_{\rm int}$, and volume should be small compared to characteristic scales of $\bar{\mathbf{G}}$ (in particular, λ), but not to the distance between $V_{\rm s}$ and $V_{\rm int}$. In free space it also follows from Eqs. (37) and (38).

The integral of $\nabla\mathbf{S}_{\rm inc}$ vanishes when integrating over A_1, as in the source-free case. Integration of the third component of the Poynting vector, $\mathbf{S}_{\rm ext}$, around the object gives the conventional extinction power:

$$\begin{aligned}W_{\rm ext} &\stackrel{\rm def}{=} -\oint_{A_1} d\mathbf{A}\cdot\mathbf{S}_{\rm ext}(\mathbf{r})\\ &= -\frac{\omega}{2}\int_{V_{\rm int}} d^3\mathbf{r}\ {\rm Im}[\mathbf{E}_{\rm inc}(\mathbf{r})\cdot\mathbf{P}^*(\mathbf{r})],\end{aligned} \tag{43}$$

where the negative sign is used in line with Eq. (29). Combining Eqs. (29), (32), (34), and (43), we obtain the classical expression commonly called the optical theorem:

$$-W_{\rm abs} = -W_{\rm ext}+W_{\rm sca} \Leftrightarrow W_{\rm ext} = W_{\rm abs}+W_{\rm sca}. \tag{44}$$

Thus, this identity holds true in the presence of sources (as soon as we assume that the sources are located outside the object). However, the expression of the scattering power in terms of forward-scattering amplitude [8] (also called the optical theorem) is only valid for a plane incident wave. By contrast, the generalized optical theorem [35], valid for any incident field, is too complicated for practical computations. Equation (44) also implies that

$$W_{\rm abs} = -\frac{\omega}{2}\int_{V_{\rm int}} d^3\mathbf{r}\ {\rm Im}[\mathbf{E}(\mathbf{r})\cdot\mathbf{P}^*(\mathbf{r})], \tag{45}$$

consistent with Eq. (29).

For scattering of the plane wave in free space it is convenient to define scattering, absorption, and extinction cross sections by normalizing corresponding power rates by intensity of the incident wave [3]. While generalization to some other incident fields is possible, e.g., to Gaussian beams [18], it is generally ambiguous, especially when impressed sources are

present. Therefore, we mostly limit the discussion to power rates instead of cross sections. Still all linear relations between power rates, like Eq. (44), can be trivially reformulated in terms of cross sections.

When the sources are present, Eq. (44) (being still correct [35]) tells only part of the story. The remaining part corresponds to the integration around V_s. The integral of $\nabla \mathbf{S}_{\rm inc}$ gives the power of radiation emitted by sources when the scatterer is absent:

$$W_0 \stackrel{\rm def}{=} \oint_{A_2} d\mathbf{A}\cdot\mathbf{S}_{\rm inc}(\mathbf{r}) = -\frac{1}{2}\int_{V_s} d^3\mathbf{r}\ {\rm Re}[\mathbf{E}_{\rm inc}(\mathbf{r})\cdot\mathbf{J}_s^*(\mathbf{r})], \quad (46)$$

which we discussed above together with potential singularities in Eqs. (19), (26), and (28). The integral of $\nabla \mathbf{S}_{\rm sca}$ vanishes, and the integral of the extinction part yields

$$W_{\rm enh} \stackrel{\rm def}{=} \oint_{A_2} d\mathbf{A}\cdot\mathbf{S}_{\rm ext}(\mathbf{r}) = -\frac{1}{2}\int_{V_s} d^3\mathbf{r}\ {\rm Re}[\mathbf{E}_{\rm sca}(\mathbf{r})\cdot\mathbf{J}_s^*(\mathbf{r})], \quad (47)$$

where we used Eq. (33) and the result is valid for any distribution of sources, even with singularities. The physical meaning of $W_{\rm enh}$ is the extra power emitted by the sources due to the presence of the object [38]. Indeed, combining Eqs. (30), (46) and (47), we obtain

$$W_{\rm em} = W_0 + W_{\rm enh}. \quad (48)$$

Alternatively, one may rewrite Eq. (31) as

$$W_{\rm rad} = W_0 + W_{\rm sca} + (W_{\rm enh} - W_{\rm ext}), \quad (49)$$

which illustrates that both $W_{\rm enh}$ and $W_{\rm ext}$ result from the interference of fields emitted by the source and scattered by the object.

Since the induced currents, proportional to $\mathbf{P}(\mathbf{r})$, are not principally different from the impressed ones with respect to the far-field radiation, we obtain

$$W_{\rm rad} = \frac{\omega\mu_0}{2}\iint_{V_s\cup V_{\rm int}} d^3\mathbf{r}d^3\mathbf{r}'[\mathbf{J}_s(\mathbf{r}) - i\omega\mathbf{P}(\mathbf{r})]^* \cdot \bar{\mathbf{G}}^I(\mathbf{r},\mathbf{r}')\cdot[\mathbf{J}_s(\mathbf{r}') - i\omega\mathbf{P}(\mathbf{r}')], \quad (50)$$

analogously to Eqs. (21) and (35). One can also introduce the far-field amplitude $\mathbf{F}_{\rm rad}$ of the total field by replacing $\mathbf{E}_{\rm sca}$, $\mathbf{F}$, $\mathbf{P}$, and $W_{\rm sca}$ in Eqs. (36)–(38) by $\mathbf{E}$, $\mathbf{F}_{\rm rad}$, $(\mathbf{P} + i\mathbf{J}_s/\omega)$, and $W_{\rm rad}$, respectively (with appropriate changes to the integration volume). In other words,

$$W_{\rm rad} = \frac{k}{2\omega\mu_0}\oint d^2\mathbf{n}\ |\mathbf{F}_{\rm rad}(\mathbf{n})|^2,\ \ \mathbf{F}_{\rm rad}(\mathbf{n}) \stackrel{\rm def}{=} \mathbf{F}_{\rm inc}(\mathbf{n}) + \mathbf{F}(\mathbf{n}). \quad (51)$$

The inconsistency of indices between $\mathbf{E}$ and $\mathbf{F}$ is caused by historically ubiquitous use of such notation for $\mathbf{F}$ (corresponding to $\mathbf{E}_{\rm sca}$) in the literature. $W_{\rm enh}$ can be computed directly from the near field using Eqs. (8), (30), and (47) [19]:

$$W_{\rm enh} = -\frac{\omega^2\mu_0}{2}{\rm Re}\left[\int_{V_s} d^3\mathbf{r}\ \mathbf{J}_s^*(\mathbf{r})\cdot\int_{V_{\rm int}} d^3\mathbf{r}'\ \bar{\mathbf{G}}(\mathbf{r},\mathbf{r}')\cdot\mathbf{P}(\mathbf{r}')\right], \quad (52)$$

where the exclusion volumes are omitted because $\mathbf{r}$ and $\mathbf{r}'$ belong to nonintersecting volumes (V_s and $V_{\rm int}$, respectively).

If all sources are in phase or exactly out of phase, i.e., $\mathbf{J}_s(\mathbf{r})e^{i\varphi}$ is a real function, and the environment is reciprocal [$\bar{\mathbf{G}}(\mathbf{r},\mathbf{r}') = \bar{\mathbf{G}}^T(\mathbf{r}',\mathbf{r})$], then Eq. (52) can be transformed to

$$\begin{aligned} W_{\rm enh} &= -\frac{\omega^2\mu_0}{2} \times {\rm Re}\left[\int_{V_{\rm int}} d^3\mathbf{r}'\ \mathbf{P}(\mathbf{r}')\cdot\int_{V_s} d^3\mathbf{r}\ \bar{\mathbf{G}}(\mathbf{r}',\mathbf{r})\cdot e^{2i\varphi}\mathbf{J}_i(\mathbf{r})\right] \\ &= -\frac{\omega}{2}\int_{V_{\rm int}} d^3\mathbf{r}\ {\rm Im}[e^{2i\varphi}\mathbf{E}_{\rm inc}(\mathbf{r})\cdot\mathbf{P}(\mathbf{r})], \end{aligned} \quad (53)$$

which is very similar to $W_{\rm ext}$ [see Eq. (43)]. The main convenience of Eq. (53) is that it requires only the knowledge of $\mathbf{E}_{\rm inc}(\mathbf{r})$ in $V_{\rm int}$ and not the sources themselves (apart from the common phase), since $\mathbf{P}(\mathbf{r})$ is also determined from $\mathbf{E}_{\rm inc}(\mathbf{r})$ through Eq. (7).

Alternatively, let us analyze the static limit of $W_{\rm enh}$ and $W_{\rm rad}$. In particular, we assume that sizes of both V_s and $V_{\rm int}$, as well as the distance between them, are smaller than all characteristic scales of $\bar{\mathbf{G}}^I(\mathbf{r},\mathbf{r}')$ (such as λ). In other words, the volume enclosing both V_s and $V_{\rm int}$ is assumed sufficiently small. Then Eq. (50) implies [see Eqs. (23) and (42)]

$$\lim_{V_s\cup V_{\rm int}\to 0} W_{\rm rad} = \frac{\omega\mu_0}{2}(\mathbf{J}_0 - i\omega\mathbf{P}_\Sigma)^*\cdot\bar{\mathbf{G}}^I(\mathbf{r}_0,\mathbf{r}_0)\cdot(\mathbf{J}_0 - i\omega\mathbf{P}_\Sigma), \quad (54)$$

i.e., the radiated power of a small system is determined by its total current (dipole moment)—a common approximation in nanophotonics [39,40]. Importantly, this does not imply any simplification in calculation of $\mathbf{P}_\Sigma$ from $\mathbf{J}_s(\mathbf{r})$; the general Eq. (7) still needs to be solved.

Unfortunately, $W_{\rm enh}$ cannot be directly simplified analogously to Eqs. (21) and (35) due to the lack of symmetry between the two vector functions on the left and right sides of $\bar{\mathbf{G}}$. However, combining it with $W_{\rm ext}$ [Eq. (43)] restores the symmetry in agreement with the physical sense of Eq. (49):

$$\begin{aligned} W_{\rm enh} - W_{\rm ext} &= -\frac{\omega^2\mu_0}{2}\int_{V_s}\int_{V_{\rm int}} d^3\mathbf{r}d^3\mathbf{r}'{\rm Re}[\mathbf{J}_s^*(\mathbf{r})\cdot\bar{\mathbf{G}}(\mathbf{r},\mathbf{r}')\cdot\mathbf{P}(\mathbf{r}') - \mathbf{P}^*(\mathbf{r}')\cdot\bar{\mathbf{G}}(\mathbf{r}',\mathbf{r})\cdot\mathbf{J}_s(\mathbf{r})] \\ &= -\omega\mu_0\int_{V_s}\int_{V_{\rm int}} d^3\mathbf{r}d^3\mathbf{r}'{\rm Re}\{\mathbf{J}_s^*(\mathbf{r})\cdot\bar{\mathbf{G}}^I(\mathbf{r},\mathbf{r}')\cdot[i\omega\mathbf{P}(\mathbf{r}')]\}, \end{aligned} \quad (55)$$

where we used Eq. (9). Taking the same limit results in

$$\lim_{V_s\cup V_{\rm int}\to 0}(W_{\rm enh} - W_{\rm ext}) = -\omega\mu_0\ {\rm Re}[\mathbf{J}_0^*\cdot\bar{\mathbf{G}}^I(\mathbf{r}_0,\mathbf{r}_0)\cdot(i\omega\mathbf{P}_\Sigma)], \quad (56)$$

which also follows from Eqs. (23), (42), (49), and (54). Therefore, even in the static limit, knowledge of $\mathbf{E}_{\rm inc}(\mathbf{r})$ in $V_{\rm int}$ is generally not sufficient, in contrast to Eq. (53). However, only the total source current $\mathbf{J}_0$ needs to be additionally known

to calculate W_{enh}, while the complex interaction between distributed $\mathbf{J}_s(\mathbf{r})$ and $\mathbf{P}(\mathbf{r})$, when the sizes of V_s and V_{int} are comparable to the distance between them, can be taken from W_{ext}.

Finally, W_{em} is closely related to the source Green's dyadic $\bar{\mathbf{G}}_s(\mathbf{r},\mathbf{r}')$, which is one of the general ways to represent the solution of the scattering problem at $\mathbf{r}$ given point-dipole excitation at $\mathbf{r}'$ [6]. It is determined solely by the scattering object (and the environment) and allows representation:

$$\mathbf{E}(\mathbf{r}) = i\omega\mu_0 \lim_{V_0\to 0}\int_{V_s\setminus V_0} d^3\mathbf{r}'\bar{\mathbf{G}}_s(\mathbf{r},\mathbf{r}')\cdot\mathbf{J}_s(\mathbf{r}') - i\frac{\mathbf{J}_s(\mathbf{r})}{3\omega\varepsilon_0}, \quad (57)$$

analogously to Eq. (9). Importantly, $\bar{\mathbf{G}}_s(\mathbf{r},\mathbf{r}') - \bar{\mathbf{G}}(\mathbf{r},\mathbf{r}')$ is regular when $\mathbf{r},\mathbf{r}' \in V_{ext}$ and, thus, is more convenient for computations. In particular, Eqs. (47) and (57) imply

$$\mathbf{E}_{sca}(\mathbf{r}) = i\omega\mu_0\int_{V_s} d^3\mathbf{r}'[\bar{\mathbf{G}}_s(\mathbf{r},\mathbf{r}') - \bar{\mathbf{G}}(\mathbf{r},\mathbf{r}')]\cdot\mathbf{J}_s(\mathbf{r}'), \quad \mathbf{r}\in V_{ext}, \quad (58)$$

$$\begin{aligned} W_{enh} &= \frac{\omega\mu_0}{2}\iint_{V_s} d^3\mathbf{r}d^3\mathbf{r}' \\ &\quad\times \mathrm{Im}\{\mathbf{J}_s^*(\mathbf{r})\cdot[\bar{\mathbf{G}}_s(\mathbf{r},\mathbf{r}') - \bar{\mathbf{G}}(\mathbf{r},\mathbf{r}')]\cdot\mathbf{J}_s(\mathbf{r}')\} \\ &= \frac{\omega\mu_0}{2}\iint_{V_s} d^3\mathbf{r}d^3\mathbf{r}' \\ &\quad\times \mathbf{J}_s^*(\mathbf{r})\cdot[\bar{\mathbf{G}}_s^I(\mathbf{r},\mathbf{r}') - \bar{\mathbf{G}}^I(\mathbf{r},\mathbf{r}')]\cdot\mathbf{J}_s(\mathbf{r}'). \end{aligned} \quad (59)$$

A simple expression for W_{em} is

$$W_{em} = \frac{\omega\mu_0}{2}\iint_{V_s} d^3\mathbf{r}d^3\mathbf{r}'\,\mathbf{J}_s^*(\mathbf{r})\cdot\bar{\mathbf{G}}_s^I(\mathbf{r},\mathbf{r}')\cdot\mathbf{J}_s(\mathbf{r}'), \quad (60)$$

$$\lim_{V_s\to 0} W_{em} = \frac{\omega\mu_0}{2}\mathbf{J}_0^*\cdot\bar{\mathbf{G}}_s^I(\mathbf{r}_0,\mathbf{r}_0)\cdot\mathbf{J}_0, \quad (61)$$

but here V_s should additionally be small compared to the distance between V_s and V_{int}, in contrast to the static limit discussed above. Equation (61) is the well-known expression for a single point source [39,41]. Comparing it to Eq. (23) one can see that the scatterer is just another component of the environment modifying the Green's dyadic, similar to a substrate discussed in Sec. IX. The discrete version of Eq. (60) has been recently discussed in [42].

VI. DECAY RATE ENHANCEMENT

Equation (48) is closely related to the interaction of the emitting system (atom, molecule, or nanoparticle) with the environment, for instance, the enhancement of fluorescence in the presence of nearby scatterers or inside a cavity, also known as the Purcell effect [10]. The emission process is quantum in nature, related to the stochastic transition of the emitter between two levels. The transition probability for a single emitter can be calculated in terms of QED. However, the quasiclassical approximation is commonly used, which we briefly describe below.

In the absence of any particles nearby, the emitters are considered as sources (usually dipoles) oscillating with damping constant γ_0 (much smaller than the resonance frequency) [38,43]. The energy of the system E (not to be confused with the electric field) thus equals

$$E(t) = E_0 e^{-\gamma_0 t} = E_0 e^{-t/\tau_0}, \quad (62)$$

where τ_0 is the lifetime of the excited state and E_0 is the initial oscillator energy. On the other hand, the energy may change over time only due to intrinsic (e.g., intramolecular) dissipation W_{in} and radiation, which gives [11]

$$\frac{dE(t)}{dt} = -\gamma_0 E_0 = -(W_0 + W_{in}) = -\frac{W_0}{q_0}, \quad (63)$$

where q_0 is the intrinsic quantum yield, i.e., the fraction of energy that is radiated, and the exponent is omitted because only the initial moment is considered. W_0 can be found using Eq. (21) as soon as the sources are defined. In terms of the QED, $q_0 \overset{\text{def}}{=} \gamma_{r0}/\gamma_0$, where γ_{r0} is the radiative decay rate, and when saying "intrinsic" we assume that both γ_{r0} and W_0 are considered for an emitter in vacuum. The apparent contrast to the general definition of Eq. (21) is discussed in Sec. IX.

When the scattering object (e.g., a nanoparticle) is present, the scattered field acts as a driving force for the oscillating sources. This results in the modified decay rate γ. Strictly speaking, E_0 also changes due to the frequency shift, but this shift is usually very small. Again, according to the energy conservation,

$$\gamma E_0 = W_{em} + W_{in}. \quad (64)$$

Assuming that W_{in} is independent of the environment, we calculate the decay rate enhancement due to the presence of the object using Eqs. (63), (64), and (48):

$$\frac{\gamma}{\gamma_0} = \frac{W_{em} + W_{in}}{W_0 + W_{in}} = 1 + q_0\frac{W_{enh}}{W_0}. \quad (65)$$

Although the sources typically emit more energy in the presence of the scatterer, this energy only partly goes to the far zone due to the absorption. Therefore, the observed fluorescence intensity may even decrease (be quenched). So it is common to separate the decay rate into the internally dissipated part $\gamma_{in} \overset{\text{def}}{=} \gamma_0 - \gamma_{r0}$, nonradiative part γ_{nr} (corresponding to the radiation absorbed in the scatterer), and radiative part γ_r (corresponding to the observable radiation) [9,19]:

$$\begin{aligned} &\gamma = \gamma_{in} + \gamma_{nr} + \gamma_r, \ \frac{\gamma_{in}}{\gamma_0} = \frac{W_{in}}{W_0 + W_{in}} = 1 - q_0, \\ &\frac{\gamma_{nr}}{\gamma_0} = q_0\frac{W_{abs}}{W_0}, \ \frac{\gamma_r}{\gamma_0} = q_0\frac{W_{rad}}{W_0}, \end{aligned} \quad (66)$$

where we used Eq. (31). The apparent quantum yield (modified by the environment) is then

$$q = \frac{\gamma_r}{\gamma} = \frac{W_{rad}}{W_{enh} + W_0/q_0} = \frac{W_{rad}}{W_{rad} + W_{abs} + W_0(1/q_0 - 1)}. \quad (67)$$

The correspondence between decay rates, apparent quantum yield, and classical power rates becomes especially simple when W_{in} can be neglected, i.e., $q_0 = 1$.

The remaining question is whether W_0 and W_{em} can be computed by the classical formulas in Sec. V. The latter

assumes that the source $\mathbf{J}_s(\mathbf{r})$, a classical representation of the quantum phenomenon of atomic or molecular emission, is impressed, i.e., independent of the environment (including the scatterer). This corresponds to a weak-coupling regime, where the transition between the excited and ground state of the emitter can be described with QED based on perturbation theory, i.e., the quantum orbitals are unaffected [9]. For instance, for the simplest two-level system without intrinsic dissipation it results in the following expression for the decay rate:

$$\gamma = \frac{\pi\omega}{\hbar\varepsilon_0}|\mathbf{p}_{eg}|^2\rho_{\mathbf{e}_0}(\mathbf{u}_0,\omega), \tag{68}$$

where $\mathbf{p}_{eg}$ is the transition dipole matrix element and $\rho_{\mathbf{e}_0}(\mathbf{u}_0,\omega)$ is the *projected LDOS*, tightly related to the source Green's dyadic (thus connecting the QED and classical description):

$$\rho_{\mathbf{e}_0}(\mathbf{u}_0,\omega) = \frac{2\omega}{\pi c^2}\big[\mathbf{e}_0\cdot\bar{\mathbf{G}}_s^I(\mathbf{u}_0,\mathbf{u}_0)\cdot\mathbf{e}_0\big], \tag{69}$$

and $\mathbf{e}_0 \overset{\text{def}}{=} \mathbf{p}_{eg}/|\mathbf{p}_{eg}|$. Alternatively, $\rho_{\mathbf{e}_0}(\mathbf{u}_0,\omega)$ is known as the partial LDOS and may include an additional factor of 3, corresponding to additional 1/3 in Eq. (68) [11]. In any case, the unambiguous quantity is the total LDOS, given in terms of Eq. (69) as

$$\rho(\mathbf{u}_0,\omega) = \frac{2\omega}{\pi c^2}\mathrm{Tr}\big[\bar{\mathbf{G}}_s^I(\mathbf{u}_0,\mathbf{u}_0)\big] = \sum_\mu \rho_{\mathbf{e}_\mu}(\mathbf{u}_0,\omega), \tag{70}$$

where $\mathbf{e}_\mu$ is the unit vector along the axis μ.

The correspondence between quantum Eqs. (68) and (69) and (quasi-) classical Eqs. (61) and (64) is exact (assuming $W_{\text{int}} = 0$), if we replace $E_0 \to \hbar\omega$ and $|\mathbf{p}_{eg}| \to |\mathbf{J}_0|/(2\omega)$, where the factor 2 appears because the Fourier transform of the classical dipole moment spans both positive and negative frequencies [11]. More importantly, irrespective of the specific constants the dependence on $\bar{\mathbf{G}}_s$ is exactly the same, justifying the calculation of decay rate enhancements through the classical power ratios—Eq. (66). The only required detail about the quantum system is q_0. Moreover, this quasiclassical result holds true when many sources are present, where quantum expression involves the *cross density of states* [9], expressed similarly to $\bar{\mathbf{G}}^I(\mathbf{r},\mathbf{r}')$ [see Eq. (22)]. It is especially surprising because the classical results follow from consideration of how the environment scatters fields, whereas in QED the same results follow from vacuum fluctuations (also depending on the environment).

Moreover, the radiative enhancement plays an important role in another ubiquitous phenomenon—SERS. Employing the quasiclassical approximation, SERS intensity can be obtained as a combination of near-field enhancement (by the scatterer) of the incident beam (e.g., a plane wave) at one frequency and enhancement of the point-dipole emission at a shifted one. The latter is directly described by the above formulas, which implicitly assume that the quantum orbitals are unaffected by the environment. Otherwise the so-called chemical mechanism of SERS become significant, which cannot be described by electrodynamics alone [12].

VII. ENERGY BUDGET IN THE DDA

This section is devoted to some computational issues arising when calculating integrals of the Poynting vector in the framework of the DDA. Once the linear system (10) is solved, polarizations for each dipole inside the object are known. Hence, all integrals in Sec. V can be approximately computed by replacing them with finite sums, and the accuracy improves with refining discretization [44]. In particular, Eqs. (29), (43), and (45) lead to

$$W_{\text{ext}} \approx -\frac{\omega}{2}\sum_i \mathrm{Im}(\mathbf{E}_{\text{inc},i}\cdot\mathbf{P}_i^*), \tag{71}$$

$$W_{\text{abs}} \approx \frac{\omega}{2}V_d\sum_i \mathrm{Im}(\varepsilon_i)|\mathbf{E}_i|^2 = -\frac{\omega}{2}\sum_i \mathrm{Im}(\mathbf{E}_i\cdot\mathbf{P}_i^*). \tag{72}$$

Calculation of scattering quantities is a bit more intricate. On one hand, direct discretization of Eqs. (35) and (37) leads to

$$W_{\text{sca}} \approx \frac{\omega^3\mu_0}{2}\sum_{i,j}\mathbf{P}_i^*\cdot\bar{\mathbf{G}}_{ij}^I\cdot\mathbf{P}_j, \tag{73}$$

$$\mathbf{F}(\mathbf{n}) \approx \frac{\omega^2\mu_0}{4\pi}(\bar{\mathbf{I}}-\mathbf{n}\otimes\mathbf{n})\cdot\sum_i \mathbf{P}_i\exp(-ik\mathbf{r}_i\cdot\mathbf{n}), \tag{74}$$

which are consistent with each other in the sense that Eq. (38) is exactly satisfied for these approximate quantities (in the free space). The simplest proof of the latter is attained by substituting $\mathbf{P}(\mathbf{r}) = \sum_i \mathbf{P}_i\delta(\mathbf{r}-\mathbf{r}_i)$ into Eqs. (35) and (37). But note that this substitution is just a convenient mathematical trick rather than the actual discretization. In Eq. (73) we used the natural extension of Eq. (22):

$$\bar{\mathbf{G}}_{ij}^I \overset{\text{def}}{=} \bar{\mathbf{G}}^I(\mathbf{r}_i,\mathbf{r}_j) = \frac{1}{2i}\big[\bar{\mathbf{G}}_{ij}-\bar{\mathbf{G}}_{ji}^H\big], \tag{75}$$

which is a 3×3 element of a $3N\times 3N$ Hermitian matrix. The latter is equal to $(-i)$ times the skew-Hermitian part of a matrix with elements $\bar{\mathbf{G}}_{ij}$; a similar matrix has been discussed in [36].

On the other hand, Eqs. (34) and (14) lead to

$$W_{\text{sca}} \approx \frac{\omega^3\mu_0}{2}\left[\sum_{\substack{i,j\\ i\neq j}}\mathbf{P}_i^*\cdot\bar{\mathbf{G}}_{ij}^I\cdot\mathbf{P}_j + \frac{1}{V_d k^2}\sum_i \mathrm{Im}(\mathbf{P}_i^*\cdot\bar{\mathbf{M}}_i\cdot\mathbf{P}_i)\right], \tag{76}$$

which is consistent with Eqs. (71) and (72), i.e., Eq. (44) is exactly satisfied. Let us further discuss the relation between Eqs. (73) and (76). They are identical if and only if

$$\bar{\mathbf{M}}_i^I = V_d k^2\bar{\mathbf{G}}_{ii}^I, \tag{77}$$

where $\bar{\mathbf{M}}_i^I \overset{\text{def}}{=} (\bar{\mathbf{M}}_i-\bar{\mathbf{M}}_i^H)/(2i)$ in accordance with Eq. (75). The identity (77) seems natural in view of Eq. (12) and corresponds to the well-known radiative-reaction correction for the dipole polarizability, given in the free space as [45]

$$\bar{\mathbf{M}}_i = i\frac{(kd)^3}{6\pi}\bar{\mathbf{I}}, \tag{78}$$

where we used Eq. (25). Moreover, many formulations for $\bar{\mathbf{M}}_i$ only add a Hermitian matrix to Eq. (78), keeping Eq. (77) valid, as discussed in [18] from a slightly different angle. In all these cases Eqs. (71) and (72) are consistent with Eq. (74), i.e., the following reformulation of the optical theorem holds exactly:

$$W_{\text{ext}} - W_{\text{abs}} = \frac{k}{2\omega\mu_0} \oint d^2\mathbf{n}\, |\mathbf{F}(\mathbf{n})|^2. \tag{79}$$

We will call such formulations of the DDA *self-consistent* with respect to the optical theorem. This is definitely a nice-to-have feature, which is closely related to the energy conservation that is often discussed for time-integration numerical schemes in various fields of science. However, this self-consistency is not an ultimate goal, since the main virtue of the numerical method is to produce the value of some quantity as accurately as possible, as compared to the (potentially unknown) exact solution. In other words, it is better to have left- and right-hand sides of Eq. (79) different but close to the exact value of W_{sca} than to have them identically equal but very far from the reference. Note that the difference between two different ways to calculate W_{sca} is always not greater than the sum of their individual errors with respect to the true value.

It has been suggested [23] to use the numerical error in Eq. (79), i.e., the difference between two different values of W_{sca}, as an internal measure of DDA accuracy. However, the above analysis shows that this suggestion is futile. For self-consistent DDA formulations the only potential errors come from the remaining residual of the iterative solution of Eq. (10) and numerical integration of $\mathbf{F}(\mathbf{n})$—both can be made (and in most simulations are) much smaller than the discretization error, caused by the finite dipole size. This iterative residual, or equivalently the difference between Eq. (73) and $W_{\text{ext}} - W_{\text{abs}}$, is also the primary cause of the "instability" visible in Fig. 1 of [36]. Even if the DDA formulation is not self-consistent, it is only marginally so, i.e., the difference between Eqs. (73) and (76) is caused only by diagonal terms, the relative contribution of which will always be small. Therefore, this numerical error may at best correlate with the actual simulation error, but cannot be used to quantitatively estimate it. To conclude, Eq. (79) is convenient for testing the programming implementation of a self-consistent DDA implementation, but is almost not related to the accuracy of the DDA itself. This agrees with our previous simulations with ADDA code [18] and is similar to the reciprocity conditions, which are automatically satisfied for the majority of the DDA formulations [46]. An open question, however, is how to make advanced DDA formulations, which modify the interaction term $\bar{\mathbf{G}}_{ij}$, self-consistent. We leave this for future research.

Calculation of energy flows related to sources, i.e., W_0, W_{enh}, W_{em}, and W_{rad}, is similar but requires further discussion of $\mathbf{J}_{\text{s}}(\mathbf{r})$. First, the singularities should be separated [see Eq. (27)], while the regular part $\mathbf{J}_{\text{r}}(\mathbf{r})$ may or may not allow analytical integration. A general $\mathbf{J}_{\text{r}}(\mathbf{r})$ may be discretized, analogously to the scatterer, into voxels replacing the integrals by sums. In the following we consider only the delta-function singularities, although the underlying equations have no limitations in this respect. In the discussed equations (with regular integration kernels) those delta functions are completely analogous to the one-point approximation of the voxels with $\mathbf{J}_i \overset{\text{def}}{=} V_{\text{ds}}\mathbf{J}_{\text{s}}(\mathbf{u}_i)$, where V_{ds} is the discretization volume for sources. Thus, we may use single indexing for the whole $\mathbf{J}_{\text{s}}$:

$$\mathbf{J}_{\text{s}}(\mathbf{r}) \approx \sum_i \mathbf{J}_i \delta(\mathbf{r} - \mathbf{u}_i), \tag{80}$$

which together with Eq. (9) implies

$$\mathbf{E}_{\text{inc},i} \approx i\omega\mu_0 \sum_i \bar{\mathbf{G}}(\mathbf{r}_i, \mathbf{u}_j) \cdot \mathbf{J}_j. \tag{81}$$

Then W_0 is approximated by the last sum in Eq. (28):

$$W_0 = \frac{\omega\mu_0}{2} \sum_{i,j} \mathbf{J}_i^* \cdot \bar{\mathbf{G}}^I(\mathbf{u}_i, \mathbf{u}_j) \cdot \mathbf{J}_j, \tag{82}$$

while W_{enh} is obtained from Eq. (52):

$$W_{\text{enh}} \approx -\frac{\omega^2\mu_0}{2} \sum_{i,j} \text{Re}[\mathbf{J}_i^* \cdot \bar{\mathbf{G}}(\mathbf{u}_i, \mathbf{r}_j) \cdot \mathbf{P}_j]. \tag{83}$$

In principle W_{em} can be obtained by discretization of Eq. (30) but that would require careful consideration of the singularities. Instead the above results can be combined using Eq. (48). The expression for W_{rad} follows from Eq. (50):

$$\begin{aligned} W_{\text{rad}} = \frac{\omega\mu_0}{2} \Bigg\{ & \sum_{i,j} \mathbf{J}_i^* \cdot \bar{\mathbf{G}}^I(\mathbf{u}_i, \mathbf{u}_j) \cdot \mathbf{J}_j \\ & + \omega^2 \sum_{i,j} \mathbf{P}_i^* \cdot \bar{\mathbf{G}}^I(\mathbf{r}_i, \mathbf{r}_j) \cdot \mathbf{P}_j \\ & + 2\omega \sum_{i,j} \text{Im}[\mathbf{J}_i^* \cdot \bar{\mathbf{G}}^I(\mathbf{u}_i, \mathbf{r}_j) \cdot \mathbf{P}_j] \Bigg\}, \end{aligned} \tag{84}$$

where the summation indices run through the full range of the corresponding arrays (different between the sums). Alternatively, Eq. (84) can be rewritten as a single double sum over the combined array $\{\mathbf{J}_1, \mathbf{J}_2 \ldots, -i\omega\mathbf{P}_1, -i\omega\mathbf{P}_2, \ldots\}$.

Interestingly, the generalized optical theorem, given by Eq. (49), is automatically satisfied in discretized form for arbitrary $\mathbf{P}_i$ (even unrelated to the DDA). Validity of Eq. (31) is additionally based on Eq. (44) and, thus, depends on the convergence of the DDA iterative solver and Eq. (77). Alternatively, W_{rad} and/or W_0 can be calculated through Eqs. (51) and (41), respectively, with $\mathbf{F}_{\text{inc}}$ given by

$$\mathbf{F}_{\text{inc}}(\mathbf{n}) \approx \frac{i\omega\mu_0}{4\pi} (\bar{\mathbf{I}} - \mathbf{n} \otimes \mathbf{n}) \cdot \sum_i \mathbf{J}_i \exp(-ik\mathbf{r}_i \cdot \mathbf{n}), \tag{85}$$

and $\mathbf{F}_{\text{rad}}$ given by a combination of Eqs. (74) and (85) [see the discussion after Eq. (74)]. Then the accuracy of the integration over the unit sphere also comes into play. In conclusion, the self-consistency of the standard DDA formulation fully extends to all variants of the generalized optical theorem in the presence of sources. However, this self-consistency vanishes if one modifies the interaction and self-terms involving $\bar{\mathbf{G}}^I$ in Eqs. (82)–(84), analogously to the advanced DDA formulations briefly mentioned above.

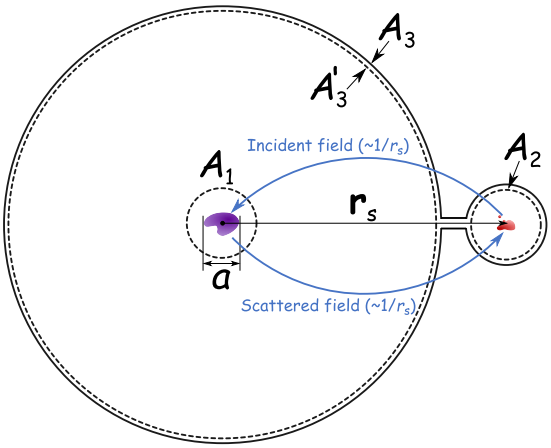

FIG. 2. Illustration of the distant source ($r_s \to \infty$); a is a characteristic scale (maximal dimension) of both the scattering object and the sources. A_1–A_3 are the same as in Fig. 1. A_3' is a part of A_3, which is a far-field limit of A_1. Blue arrows indicate that both incident and scattered waves are in the far zone near the object and the sources, respectively.

Finally, if all $\mathbf{J}_i$ are in phase, Eq. (53) implies

$$W_{\rm enh} \approx -\frac{\omega}{2}\sum_i \mathrm{Im}[e^{2i\varphi}\mathbf{E}_{{\rm inc},i}\cdot\mathbf{P}_i]. \tag{86}$$

In particular, if the source is a single point dipole with real dipole moment $\mathbf{p}_0$ then $e^{2i\varphi} = -1$. The resulting formula is currently used in the ADDA code [18]. Note that the enhancement factor $W_{\rm enh}/W_0$ is independent of $\mathbf{p}_0$ (but depends on the dipole position).

VIII. INFINITELY DISTANT SOURCES

An important practical case is the incident wave that propagates from infinity, which physically corresponds to the sources situated far from the object. The limit of Eqs. (5), (8), and (9) when the pointlike source is situated in a far zone was derived in [6,7] and coincides with the conventional light-scattering problem under plane-wave illumination. Other solutions of homogeneous Maxwell's equations, like Gaussian [47], Bessel [48], and Airy beams [49], also correspond to the appropriate distribution of sources at infinity (on a sphere with infinitely large radius). For brevity we denote all these cases as source-free ones, and limit ourselves to the free-space case, since otherwise the particular details of the environment are essential for taking the following limits.

Let us look at the integrals from Secs. IV and V when the distance between $V_{\rm int}$ and $V_{\rm s}$ (the object and the sources) $r_{\rm s} = |\mathbf{r}_{\rm s}|$ is large compared to their characteristic dimensions a (Fig. 2), so that each one is in the far-field zone of the other:

$$kr_{\rm s} \gg 1,\ kr_{\rm s} \gg (ka)^2, \tag{87}$$

which obviously implies $r_{\rm s} \gg a$. In doing so we need to be careful about the order of limits. Since we previously assumed that the surface A_3 encloses both the source and the scatterer (Fig. 1), it should expand with increasing $r_{\rm s}$. To separate the limiting processes, we deformed A_3 as shown in Fig. 2, which is equivalent to separating it into A_2 and A_3'. The latter is equivalent to A_1 but is in the far field of the scatterer.

Let us first consider $V_{\rm s}$ of a fixed size, then the source-generated field near the object in the free space is locally a plane wave [6]:

$$\mathbf{E}_{\rm inc}(\mathbf{r}) \underset{r_{\rm s}\to\infty}{\to} \mathbf{E}_0 \exp(ik\mathbf{n}_{\rm inc}\cdot\mathbf{r}),\ \mathbf{r}\in V_{\rm int}, \tag{88}$$

where $\mathbf{n}_{\rm inc} \overset{\rm def}{=} -\mathbf{r}_{\rm s}/r_{\rm s}$ is the propagation direction and the amplitude

$$\mathbf{E}_0 = \frac{1}{r_{\rm s}}\mathbf{F}_{\rm inc}(\mathbf{n}_{\rm inc}) \tag{89}$$

[see Eq. (40)]. Further, we assume that $\mathbf{E}_0$ is fixed (for direct correspondence with the plane-wave incidence), while the distribution of sources moves as a whole with a common scaling by a complex factor. In other words,

$$\mathbf{J}_{\rm s}(\mathbf{r}) = r_{\rm s}\exp(-ikr_{\rm s})\mathbf{J}_{\rm s}^{(0)}(\mathbf{r}-\mathbf{r}_{\rm s}), \tag{90}$$

where the function $\mathbf{J}_{\rm s}^{(0)}$ is independent of $r_{\rm s}$. Then,

$$\mathbf{E}_0 = \frac{i\omega\mu_0}{4\pi}(\bar{\mathbf{I}} - \mathbf{n}_{\rm inc}\otimes\mathbf{n}_{\rm inc}) \cdot \int_{V_{\rm s}} d^3\mathbf{r}\exp[-ik(\mathbf{r}-\mathbf{r}_{\rm s})\cdot\mathbf{n}_{\rm inc}]\mathbf{J}_{\rm s}^{(0)}(\mathbf{r}-\mathbf{r}_{\rm s}), \tag{91}$$

which is indeed independent of $r_{\rm s}$. According to Eq. (21), the emission power scales quadratically with $r_{\rm s}$:

$$W_0 = r_{\rm s}^2\frac{\omega\mu_0}{2}\iint_{V_{\rm s}} d^3\mathbf{r}\,d^3\mathbf{r}' \times \mathbf{J}_{\rm s}^{(0)*}(\mathbf{r}-\mathbf{r}_{\rm s})\cdot\bar{\mathbf{G}}^I(\mathbf{r},\mathbf{r}')\cdot\mathbf{J}_{\rm s}^{(0)}(\mathbf{r}'-\mathbf{r}_{\rm s}), \tag{92}$$

By contrast, $\mathbf{E}_{\rm inc}(\mathbf{r})$, $\mathbf{E}(\mathbf{r})$, and $\mathbf{P}(\mathbf{r})$ inside the scatterer and all derived quantities [$\mathbf{F}(\mathbf{n})$, $W_{\rm ext}$, $W_{\rm abs}$, and $W_{\rm sca}$] do not depend on $r_{\rm s}$, leading to the following scattered field in $V_{\rm s}$ [see Eq. (36)]:

$$\mathbf{E}_{\rm sca}(\mathbf{r}) \underset{r_{\rm s}\to\infty}{\to} \frac{\exp(ikr_{\rm s})}{r_{\rm s}}\exp[ik(\mathbf{r}_{\rm s}-\mathbf{r})\cdot\mathbf{n}_{\rm inc}]\mathbf{F}(-\mathbf{n}_{\rm inc}), \tag{93}$$

where the limit denotes the asymptotic. Hence, Eq. (47) leads to

$$W_{\rm enh} \underset{r_{\rm s}\to\infty}{\to} -\frac{1}{2}\mathrm{Re}\left\{\exp(2ikr_{\rm s})\mathbf{F}(-\mathbf{n}_{\rm inc}) \cdot\int_{V_{\rm s}} d^3\mathbf{r}\exp[-ik(\mathbf{r}-\mathbf{r}_{\rm s})\cdot\mathbf{n}_{\rm inc}]\mathbf{J}_{\rm s}^{(0)*}(\mathbf{r}-\mathbf{r}_{\rm s})\right\}. \tag{94}$$

The remaining integral is different from that in Eq. (91) by conjugation of current, but is also independent of $r_{\rm s}$. Thus, $W_{\rm enh}$ oscillates with $r_{\rm s}$ but stays $\mathcal{O}(1)$, which is related to backscattering interference.

Hence, the presence of the object enhances the emission power of sources, even if they are at large distance; but this enhancement is negligible compared to the total emission power:

$$\frac{W_{\rm enh}}{W_0} = \mathcal{O}(r_{\rm s}^{-2}) \underset{r_{\rm s}\to\infty}{\to} 0,\quad \frac{W_{\rm em}}{W_0} = 1 + \frac{W_{\rm enh}}{W_0} \underset{r_{\rm s}\to\infty}{\to} 1. \tag{95}$$

Therefore, Eq. (49) is still valid, but contains infinities on both sides ($W_{\rm rad}/W_0 \underset{r_{\rm s}\to\infty}{\to} 1$). The meaningful part of it is exactly

Eq. (44), where all quantities are independent of r_s. The same result is obtained if we interchange the limits and first let $r_s \to \infty$, thus moving the sources out of all integration surfaces. In this case A_3 is replaced by A_3' (Fig. 2) and the whole energy budget boils down to Eq. (44)—a classical result for the source-free case.

Let us further discard the requirement of finiteness of V_s. Instead we consider the sources that are distributed on a sphere with radius r_s and stretch with it. Analogously to Eq. (90) we assume that

$$\mathbf{J}_s(\mathbf{r}) = \frac{\exp(-ikr_s)}{r_s}\delta(r - r_s)\mathbf{J}_s^{(0)}(\mathbf{n}_{inc}), \tag{96}$$

leading to r_s-independent incident field [7]

$$\mathbf{E}_{inc}(\mathbf{r}) \underset{r_s\to\infty}{\to} \frac{i\omega\mu_0}{4\pi}\oint d^2\mathbf{n}\ \exp(ik\mathbf{n}\cdot\mathbf{r}) \times (\bar{\mathbf{I}} - \mathbf{n}\otimes\mathbf{n})\cdot\mathbf{J}_s^{(0)}(\mathbf{n}),\ \mathbf{r}\in V_{int}, \tag{97}$$

where we omitted the subscript "inc" of $\mathbf{n}$ for simplicity. Note that the scatterer is in the far field of each differential component of $\mathbf{J}_s^{(0)}(\mathbf{n})$, but not for the whole V_s. Equation (97) is exactly the angular-spectrum representation commonly used for various nonplane beams [48].

Analogously to Eq. (92) we obtain

$$W_0 = r_s^2\frac{\omega\mu_0}{2}\oint\oint d^2\mathbf{n}\, d^2\mathbf{n}'\, \mathbf{J}_s^{(0)*}(\mathbf{n})\cdot\bar{\mathbf{G}}^I(r_s\mathbf{n}, r_s\mathbf{n}')\cdot\mathbf{J}_s^{(0)}(\mathbf{n}'), \tag{98}$$

but further analysis requires us to discuss the details of $\mathbf{J}_s^{(0)}(\mathbf{n})$. Fundamentally, the main complication comes from interweaving two limiting processes: $r_s \to \infty$ and potential singularities of $\mathbf{J}_s^{(0)}(\mathbf{n})$, e.g., $\mathbf{J}_s^{(0)}(\mathbf{n}) \to \delta(\mathbf{n} - \mathbf{n}_0)$. First, consider the case of a finite number of point sources [see Eq. (27)]:

$$\mathbf{J}_s^{(0)}(\mathbf{n}) = \sum_i \mathbf{J}_i^{(0)}\delta(\mathbf{n} - \mathbf{n}_i). \tag{99}$$

In particular, the case of a single source corresponds to Eq. (90), keeping in mind that $\delta(r - r_s)\delta(\mathbf{n} - \mathbf{n}_i) = r_s^2\delta(\mathbf{r} - r_s\mathbf{n}_i)$. Equation (99) corresponds to taking the singular limit first, leading to

$$W_0 = r_s^2\frac{\omega\mu_0}{2}\sum_{i,j}\mathbf{J}_i^{(0)*}\cdot\bar{\mathbf{G}}^I(r_s\mathbf{n}_i, r_s\mathbf{n}_j)\cdot\mathbf{J}_j^{(0)} \underset{r_s\to\infty}{\to} r_s^2\frac{\omega^2\mu_0}{12\pi c}\sum_i\left|\mathbf{J}_i^{(0)}\right|^2, \tag{100}$$

where we used the decay of $\bar{\mathbf{G}}^I$ at large arguments [see Eq. (A6)]. In other words, the point sources do not affect each other.

The behavior of W_0 is markedly different in the opposite case of smooth $\mathbf{J}_s^{(0)}(\mathbf{n})$, i.e., when the limit $r_s \to \infty$ is taken first. An explicit derivation in the Appendix [Eq. (A10)] leads to the bounded W_0, the detailed discussion of which is outside the scope of this paper. However, we believe that such smooth distribution of sources on a large spherical shell is less physically relevant. For instance, if one considers the angular spectrum representation of a beam, those sources—located on a surface of a distant lens—are *virtual* ones, caused by real sources located behind the optical system. And calculating either W_0 or W_{enh} makes no sense for the virtual sources. Alternatively, a real source of such large extent is expected to be not fully coherent. If we assume a fixed coherence length, the distributed source will be qualitatively similar to a number of small sources incoherent and separated from each other. In the limit $r_s \to \infty$ each source is seen as a point one, while their number increases—this case is described by Eqs. (99) and (100).

The enhanced power for arbitrary $\mathbf{J}_s^{(0)}(\mathbf{n})$ is

$$W_{enh} \underset{r_s\to\infty}{\to} -\frac{1}{2}\mathrm{Re}\left[\exp(2ikr_s)\oint d^2\mathbf{n}\ \mathbf{F}(-\mathbf{n})\cdot\mathbf{J}_s^{(0)*}(\mathbf{n})\right], \tag{101}$$

which is related to the expression for W_{ext} in terms of $\mathbf{F}(\mathbf{n})$ for the same incident field [35] [see Eqs. (43) and (97)]. Importantly, when Eq. (99) specifies the sources, Eq. (95) is still valid together with all the discussion around it. The only change is required in the source-related part of A_3 (or A_2) in Fig. 2—it should be stretched into a spherical shell enclosing the source-supporting sphere, being more distant than A_3'.

Even more general distribution of distant sources can be considered by adding a radial distribution to Eq. (96), keeping Eq. (99) satisfied. However, it results in $\mathbf{E}_{inc}(\mathbf{r})$ exactly representable by Eq. (97) with another effective $\mathbf{J}_s^{(0)}(\mathbf{n})$; the same equivalence applies to all scatterer-related quantities. Expressions for W_0 and W_{enh} are more complicated [combinations of Eqs. (92) and (98) and Eqs. (94) and (101), respectively], but Eq. (95) remains unchanged.

Finally, let us briefly comment on the incident field generated by the moving electron, relevant for the EELS and cathodoluminescence [15]. The corresponding frequency-domain sources are distributed along the electron trajectory, including parts both near to and infinitely far from the scatterer. This complicates the rigorous consideration of limits and integration surfaces, which we leave for future research. However, all formulas of Sec. V apply since the integrals over the infinite V_s are well defined, and are already used for practical simulations [13,14].

IX. PRESENCE OF A PLANAR SUBSTRATE

In many experimental techniques and applications, especially in nanophotonics, a quantum emitter and/or scattering objects are located near a plane surface. The substrate alters both emission of the sources and its interaction with scatterers. In this section we deal with corresponding power integrals. Although we assume a planar substrate to keep the discussion specific, most of the discussion can be extended to other environments.

Fortunately, the presence of a substrate can be taken into account by the modification of Green's dyadic making most of the previous results valid without any modifications. In particular, the VIE framework of Eq. (5) remains unchanged, but $\bar{\mathbf{G}}(\mathbf{r}, \mathbf{r}')$ is no longer given by Eq. (6). The incident field either is expressed by the same Eq. (9) or needs simple modification by reflection and transmission if it is given by a plane wave [see Eq. (88)]. The latter can also be obtained automatically by taking the proper far-field limit of $\bar{\mathbf{G}}(\mathbf{r}, \mathbf{r}')$. This VIE framework forms the foundation of the efficient

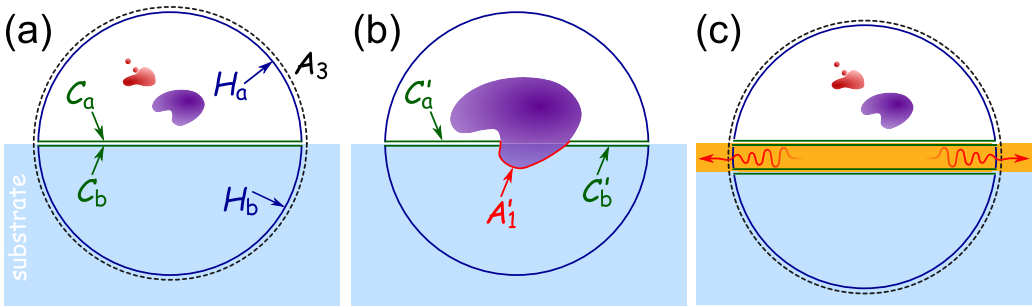

FIG. 3. (a) Division of the integration sphere into the upper and lower halves allows one to avoid field discontinuities at the interface. (b) Extra definitions of integration surfaces for the partly immersed scatterer. (c) A multilayered substrate may contain a planar waveguide, leading to an additional channel of energy transfer. See the text for explanation.

numerical methods (see, e.g., the DDA [50]). Note that the actual calculation of $\bar{\mathbf{G}}(\mathbf{r},\mathbf{r}')$, related to the Sommerfeld integrals [51,52], is far from trivial even in the case of a semi-infinite plane homogeneous substrate, especially when relevant values of $\mathbf{r}$ and $\mathbf{r}'$ are on different sides of the surface.

When turning to the energy balance of the obtained solution, the results of Secs. IV–VI are still valid (unless the free-space case was explicitly mentioned), but a number of complications appear, which are discussed in the following. The first issue is related to integration surfaces in Fig. 1. Previously we freely deformed them with the only requirement being to intersect neither the scatterer nor the sources. Now the additional boundary is that of the substrate. Let us, first, consider that the sources and the scatterer are above the substrate [Fig. 3(a)]. Then A_1 and A_2 require no extra attention, while A_3 can, formally, be extended only down to the substrate, corresponding to $S_a \stackrel{\text{def}}{=} H_a \cup C_a$, where H_a, H_b and C_a, C_b are hemispheres and circular plane caps above and below the substrate, respectively. Therefore, we modify the definition of W_{rad} to

$$W_{\text{rad}} \stackrel{\text{def}}{=} W_{\text{em}} - W_{\text{abs}} = \oint_{S_a} d\mathbf{A}\cdot\mathbf{S}(\mathbf{r}) \tag{102}$$

[see Eq. (31)]. Although this slightly changes the physical meaning of W_{rad} (see below), it allows us to keep the volume-integral expressions for W_{rad} [Eq. (50)] and its components from Fig. 1—Eqs. (21), (29), (30), (35), (43), and (47), as well as all relations between them.

Let us additionally define the absorption power inside the substrate (environment):

$$W_{\text{abs}}^{\text{env}} \stackrel{\text{def}}{=} \frac{\omega}{2}\int_{V_{\text{env}}} d^3\mathbf{r}\,|\mathbf{E}(\mathbf{r})|^2 \text{Im}[\varepsilon_{\text{env}}(\mathbf{r})] = -\oint_{S_b} d\mathbf{A}\cdot\mathbf{S}(\mathbf{r}), \tag{103}$$

where V_{env} includes all absorbing parts of the substrate, $S_b \stackrel{\text{def}}{=} H_b \cup C_b$, and the radius of H_b is assumed infinitely large. Next, we use the continuity of the normal components of $\mathbf{S}(\mathbf{r})$ across the interface (due to the boundary conditions for the tangential components of the fields), implying

$$\iint_{C_a} d\mathbf{A}\cdot\mathbf{S}(\mathbf{r}) = -\iint_{C_b} d\mathbf{A}\cdot\mathbf{S}(\mathbf{r}), \tag{104}$$

where the minus appears due to the opposite directions of normal. Coming back to A_3, defined as a very large sphere [Fig. 3(a)], we can calculate the total radiated power *going to infinity*:

$$W_{\text{rad}}^{\infty} \stackrel{\text{def}}{=} \oint_{A_3} d\mathbf{A}\cdot\mathbf{S}(\mathbf{r}) = W_{\text{em}} - W_{\text{abs}} - W_{\text{abs}}^{\text{env}}, \tag{105}$$

where the second equality follows from Eqs. (102)–(104) and is also consistent with general energy conservation.

The situation is more complicated when the scatterer is partly immersed in the substrate [see Fig. 3(b)]. Let us exclude the parts of C_a and C_b intersecting the scatterer ($C'_{a,b} \stackrel{\text{def}}{=} C_{a,b}\backslash V_{\text{int}}$) and define the scatterer boundary inside the substrate as A'_1. Then the above results stay the same if we deform $S_{a,b}$ into $H_{a,b}\cup C'_{a,b}\cup A'_1$ and assume that V_{env} excludes the immersed part of the scatterer. Note, however, that the used $\bar{\mathbf{G}}(\mathbf{r},\mathbf{r}')$ corresponds to a complete semi-infinite substrate, which should be accounted for in the VIE. Formulation of Eq. (7) remains identical, but $\mathbf{P}(\mathbf{r}) \stackrel{\text{def}}{=} [\varepsilon(\mathbf{r})-\varepsilon_{\text{env}}(\mathbf{r})]\mathbf{E}(\mathbf{r})$. This generalized VIE together with Eq. (105) and the first part of Eq. (103) are expected to be valid for a wide range of complicated environments, at least for those where the far-field limit has some physical sense (e.g., not for a closed cavity). Moreover, the sources can also be located inside the medium of the environment. However, the corresponding rigorous analysis is beyond the scope of this paper.

Considering the simulations of energy flows for a homogeneous substrate, e.g., in the framework of the DDA, the direct calculation of $W_{\text{abs}}^{\text{env}}$ (if not zero) has larger computational complexity than that of W_{em} and W_{abs}. Although, after replacing S_b by $-C_a$ in Eq. (103), it requires only values of $\bar{\mathbf{G}}(\mathbf{r},\mathbf{r}')$ with $\mathbf{r}$ on the interface (presumably simpler to compute), an even simpler option is to compute W_{rad}^{∞} directly in the far-field zone (in contrast to the free-space case). In most cases the integration may be limited to H_a, e.g., $W_{\text{rad}}^{\infty} = W_{\text{rad}}^{a}$, where

$$W_{\text{rad}}^{a} \stackrel{\text{def}}{=} \oint_{H_a} d\mathbf{A}\cdot\mathbf{S}(\mathbf{r}), \tag{106}$$

but one may also consider a finite substrate (e.g., a hemisphere) with very small absorption that is large enough to use half-space expressions for $\bar{\mathbf{G}}(\mathbf{r},\mathbf{r}')$ but not large enough to completely absorb the radiation scattered into it. If the substrate is nonabsorbing, the total $W_{\text{rad}}^{\infty} = W_{\text{rad}}$ is obtained automatically, but many experimental configurations measure only W_{rad}^{a} (in the upper hemisphere), which requires separate calculation unless the substrate is perfectly conducting.

Fortunately, the far-field limit of $\bar{\mathbf{G}}(\mathbf{r},\mathbf{r}')$ is not much more involved than that in the free space. Thus, we can use the same integral over the unit sphere, Eq. (51), but with k dependent on $\mathbf{n}$ and the scattering amplitudes including reflected and transmitted terms (see, e.g., the Supporting Information of Ref. [50]). The integrand is commonly zero (and, thus, continuous) at the substrate interface [53], but not for multilayered substrates, which include a dielectric planar waveguide [Fig. 3(c)]. The latter channel the energy at the polar angle equal to exactly $\pi/2$ [11,54] (with respect to substrate normal) and require extra fragmentation of integration surfaces. In the waveguide $\mathbf{S}(\mathbf{r})$ scales as r^{-1}, in contrast to r^{-2} elsewhere, leading to delta-function dependence of $|\mathbf{F}_{\rm rad}(\mathbf{n})|^2$ at exactly oblique direction. The integral over the unit sphere is still well defined, but it is ambiguous whether this delta-function contribution should be included in $W^{\rm a}_{\rm rad}$. The latter ultimately depends on the specific measurement conditions. Additional simplifications for $W_{\rm ext}$ are possible for the plane-wave excitation [53,55], similar to the free-space case.

Finally, let us discuss the decay rate enhancements. In principle, all formulas in Sec. VI are still valid, but a few ambiguities appear. The first question is what is exactly the radiative part of the enhancement (i.e., the "useful" part). Depending on the application (see above), $W_{\rm rad}$ in Eqs. (66) and (67) may need to be replaced by $W^{\infty}_{\rm rad}$ or $W^{\rm a}_{\rm rad}$, while $W_{\rm abs}$ may need to be replaced by $W_{\rm abs}+W^{\rm env}_{\rm abs}$ or by $W_{\rm em}-W^{\rm a}_{\rm rad}$, respectively. The second question is what is the original state to compare with—either free space or environment without the scatterer. To keep using the intrinsic quantum yield q_0, we need to replace W_0 by $W^{\rm fr}_0$, given by Eq. (20) with the free-space Green's dyadic. Then W_0 will correspond to the decay rate in the environment $\gamma_{\rm env}$, in contrast to the free-space γ_0, but this emitted power does not necessarily entirely go to infinity. In the following we list the generalized formulas, valid for an arbitrary environment:

$$\frac{\gamma_{\rm env}}{\gamma_0}=\frac{W_0}{W^{\rm fr}_0+W_{\rm in}}=q_0\frac{W_0}{W^{\rm fr}_0}, \tag{107}$$

$$\frac{\gamma}{\gamma_0}=1+q_0\left(\frac{W_{\rm em}}{W^{\rm fr}_0}-1\right),\quad \frac{\gamma_{\rm nr}}{\gamma_0}=q_0\frac{W_{\rm abs}+W^{\rm env}_{\rm abs}}{W^{\rm fr}_0},$$

$$\frac{\gamma_{\rm r}}{\gamma_0}=q_0\frac{W^{\infty}_{\rm rad}}{W^{\rm fr}_0}, \tag{108}$$

$$q=\frac{\gamma_{\rm r}}{\gamma}=\frac{W^{\infty}_{\rm rad}}{W_{\rm em}+W^{\rm fr}_0(1/q_0-1)}. \tag{109}$$

Enhancement relative to $\gamma_{\rm env}$ can be obtained by dividing Eq. (108) by Eq. (107), and $W^{\infty}_{\rm rad}$ can be adjusted to include only the detectable radiation (depending on a specific application).

X. CONCLUSION

We outlined a rigorous approach to treat electromagnetic energy flows in the frequency-domain light-scattering problem with explicit sources. Starting from the VIE formulation of Maxwell's equation, we considered the flow of the Poynting vector through different surfaces, including complex geometries in the presence of a substrate. This led to the energy-balance equations, generalizing the concepts of optical cross sections and the optical theorem. We showed the relevance of these energy-balance equations to the measurable quantities in nanophotonics, such as the enhancement of atomic or molecular emission and corresponding decay rates by a nanoparticle. The concepts of radiative and nonradiative parts of decay rate enhancement have been generalized to nanoparticles near a planar substrate. This should lead to a wider usage of those parts in contrast to the first papers, where only the total enhancement was calculated without any approximations [21]. We paid special attention to the practical calculation of the power rates and decay rate enhancements in the framework of the DDA, substantiating some formulas that are already used in a production code [18]. Moreover, we showed that the conventional optical theorem is automatically satisfied for most of the DDA formulations and, thus, cannot be used as an internal measure of the DDA accuracy.

Apart from filling the essential gap in the existing literature the resulting description is reasonably self-contained and complete, covering the energy budget of the VIE with impressed sources from all possible perspectives. As such, this paper can also be considered a state-of-the-art review of this subject. Moreover, the definitions of power rates and interrelations between them are applicable to any mathematical formulation of the frequency-domain scattering problem, e.g., based on differential or surface-integral equations, and to corresponding numerical methods. The paper may also contribute to bringing closer the communities working with conventional far-field light scattering and applications involving source-induced fields.

With regards to future research, it is desirable to extend this analysis to anisotropic and magnetic materials. The energy-budget concepts remain valid, but consideration of magnetic materials would require replacing a single VIE with a system of two coupled VIEs, for the electric and magnetic fields, respectively. This would require modification of all formulas that express power rates through the fields inside the scattering object. Another interesting generalization is that of nonreciprocal environment and/or scatterer. We have mostly avoided this assumption [see Eq. (22)], but it remains to be seen if nonreciprocity leads to any new features with respect to the energy budget.

ACKNOWLEDGMENTS

We thank Michael Mishchenko for stimulating discussions that motivated us to finalize this paper and two anonymous reviewers for thorough and constructive comments. The work was supported by the Russian Science Foundation (Grant No. 18-12-00052).

APPENDIX

In the following we explicitly derive Eq. (39). First, we calculate the following for arbitrary real $\mathbf{a}$:

$$\frac{1}{4\pi}\oint d^2\mathbf{n}\exp(i\mathbf{a}\cdot\mathbf{n})=\frac{1}{2}\int_{-1}^{1}d\xi\exp(ia\xi)=\frac{\sin a}{a}, \tag{A1}$$

where we chose the z axis of the spherical coordinate system along $\mathbf{a}$, making the integrand independent of azimuthal angle

φ, and $\xi \stackrel{\text{def}}{=} \cos\theta$, where θ is the polar angle. Second, we define the projection dyadics parallel and perpendicular to $\mathbf{a}$:

$$\bar{\mathbf{I}}_\parallel \stackrel{\text{def}}{=} \frac{\mathbf{a}\otimes\mathbf{a}}{a^2},\ \bar{\mathbf{I}}_\perp \stackrel{\text{def}}{=} \bar{\mathbf{I}} - \bar{\mathbf{I}}_\parallel, \tag{A2}$$

which separate $\mathbf{n}$ into two parts:

$$\mathbf{n}_\parallel \stackrel{\text{def}}{=} \bar{\mathbf{I}}_\parallel\mathbf{n} \Rightarrow \mathbf{n}_\parallel\otimes\mathbf{n}_\parallel = n_\parallel^2\bar{\mathbf{I}}_\parallel,\quad \mathbf{n}_\perp \stackrel{\text{def}}{=} \bar{\mathbf{I}}_\perp\mathbf{n} \Rightarrow \mathbf{n} = \mathbf{n}_\parallel + \mathbf{n}_\perp,\ n_\parallel^2 + n_\perp^2 = 1. \tag{A3}$$

Then in the same spherical coordinate system,

$$\frac{1}{2\pi}\int_0^{2\pi} d\varphi\mathbf{n}\otimes\mathbf{n} = \mathbf{n}_\parallel\otimes\mathbf{n}_\parallel + \frac{1}{2\pi}\int_0^{2\pi} d\varphi\mathbf{n}_\perp\otimes\mathbf{n}_\perp = n_\parallel^2\bar{\mathbf{I}}_\parallel + \frac{1}{2}n_\perp^2\bar{\mathbf{I}}_\perp = \frac{1}{2}[n_\parallel^2(3\bar{\mathbf{I}}_\parallel - \bar{\mathbf{I}}) + \bar{\mathbf{I}}_\perp], \tag{A4}$$

where the nondiagonal terms (linear in $\mathbf{n}_x$ and/or $\mathbf{n}_y$) vanish due to the symmetry of the integration interval, and $1/2$ is the result of averaging of $\cos^2\varphi$ and $\sin^2\varphi$.

Third, we calculate

$$\frac{1}{4\pi}\oint d^2\mathbf{n}\exp(i\mathbf{a}\cdot\mathbf{n})\mathbf{n}\otimes\mathbf{n} = \frac{1}{4}\int_{-1}^{1} d\xi\exp(ia\xi)[\xi^2(3\bar{\mathbf{I}}_\parallel - \bar{\mathbf{I}}) + \bar{\mathbf{I}}_\perp] = \frac{\sin a}{a}\bar{\mathbf{I}}_\parallel + \frac{a\cos a - \sin a}{a^3}(3\bar{\mathbf{I}}_\parallel - \bar{\mathbf{I}}), \tag{A5}$$

where we employed integration by parts twice. Combining Eqs. (A1) and (A5) we obtain

$$\begin{aligned}\frac{k}{(4\pi)^2}\oint d^2\mathbf{n}\exp(ik(\mathbf{r}-\mathbf{r}')\cdot\mathbf{n})(\bar{\mathbf{I}} - \mathbf{n}\otimes\mathbf{n}) &= \frac{1}{4\pi R}\left[\sin(kR)\left(\bar{\mathbf{I}} - \frac{\mathbf{R}\otimes\mathbf{R}}{R^2}\right) + \frac{kR\cos(kR) - \sin(kR)}{(kR)^2}\left(\bar{\mathbf{I}} - 3\frac{\mathbf{R}\otimes\mathbf{R}}{R^2}\right)\right]\\ &= \bar{\mathbf{G}}^I(\mathbf{r},\mathbf{r}'),\end{aligned} \tag{A6}$$

where $\mathbf{R} = \mathbf{r} - \mathbf{r}'$, and the last equality is a trivial implication of Eq. (6). Finally, let us expand $\bar{\mathbf{G}}^I(\mathbf{r},\mathbf{r}')$ for small R:

$$\bar{\mathbf{G}}^I(\mathbf{r},\mathbf{r}') = \frac{k}{6\pi}\left\{\bar{\mathbf{I}} - \frac{(kR)^2}{10}\left(2\bar{\mathbf{I}} - \frac{\mathbf{R}\otimes\mathbf{R}}{R^2}\right) + \mathcal{O}[(kR)^4]\right\}. \tag{A7}$$

Mind, however, that Eqs. (A6) and (A7) are valid only in the free space.

In the second part of the Appendix we evaluate W_0 for distant shells of sources with smooth density, i.e., Eq. (98) with *smooth* $\mathbf{J}_\mathrm{s}^{(0)}(\mathbf{n})$. For that we consider the inner integral over $\mathbf{n}'$, set the z axis of the coordinate system of $\mathbf{n}'$ (with spherical angles θ and φ) along $\mathbf{n}$, and define $x_\mathrm{s} \stackrel{\text{def}}{=} kr_\mathrm{s}$ and $\mathbf{v} \stackrel{\text{def}}{=} \mathbf{n}' - \mathbf{n}$. The latter implies $v = 2\sin(\theta/2)$ and $\sin\theta d\theta = vdv$, leading to

$$\begin{aligned}r_\mathrm{s}^2\oint d^2\mathbf{n}'\bar{\mathbf{G}}^I(r_\mathrm{s}\mathbf{n}, r_\mathrm{s}\mathbf{n}')\cdot\mathbf{J}_\mathrm{s}^{(0)}(\mathbf{n}') &= \frac{x_\mathrm{s}}{4\pi k}\int_0^2 dv\left[\sin(x_\mathrm{s}v)g_1(v) + \frac{x_\mathrm{s}v\cos(x_\mathrm{s}v) - \sin(x_\mathrm{s}v)}{(x_\mathrm{s}v)^2}g_2(v)\right]\\ &= \frac{1}{4\pi k}\left[-\cos(x_\mathrm{s}v)g_1(v) + \frac{\sin(x_\mathrm{s}v)}{x_\mathrm{s}v}g_2(v)\right]\Bigg|_{v=0}^{v=2} + \mathcal{O}\left(\frac{1}{x_\mathrm{s}}\right)\\ &= \frac{1}{4\pi k}\left[g_1(0) - g_2(0) - \cos(2x_\mathrm{s})g_1(2)\right] + \mathcal{O}\left(\frac{1}{x_\mathrm{s}}\right),\end{aligned} \tag{A8}$$

where we used integration by parts, and

$$g_1(v) \stackrel{\text{def}}{=} \int_0^{2\pi} d\varphi\left(\bar{\mathbf{I}} - \frac{\mathbf{v}\otimes\mathbf{v}}{v^2}\right)\mathbf{J}_\mathrm{s}^{(0)}(\mathbf{n}'),\quad g_2(v) \stackrel{\text{def}}{=} \int_0^{2\pi} d\varphi\left(\bar{\mathbf{I}} - 3\frac{\mathbf{v}\otimes\mathbf{v}}{v^2}\right)\mathbf{J}_\mathrm{s}^{(0)}(\mathbf{n}'). \tag{A9}$$

When $v\to 0$, $\mathbf{v}\otimes\mathbf{v}/v^2$ averages to half the projector perpendicular to $\mathbf{n}$, similar to the second integral in Eq. (A4); thus, it can be replaced by $(\bar{\mathbf{I}} - \mathbf{n}\otimes\mathbf{n})/2$. By contrast, $\mathbf{v} = -2\mathbf{n}$ (independent of φ) when $v = 2$. Substituting Eq. (A9) into Eq. (98) we obtain

$$W_0 \underset{r_\mathrm{s}\to\infty}{\to} \frac{\mu_0 c}{4}\oint d^2\mathbf{n}\ \mathbf{J}_\mathrm{s}^{(0)*}(\mathbf{n})\cdot(\bar{\mathbf{I}} - \mathbf{n}\otimes\mathbf{n})\cdot\left[\mathbf{J}_\mathrm{s}^{(0)}(\mathbf{n}) - \cos(2kr_\mathrm{s})\mathbf{J}_\mathrm{s}^{(0)}(-\mathbf{n})\right], \tag{A10}$$

i.e., W_0 oscillates with r_s but stays $\mathcal{O}(1)$ [see Eq. (94)]. We stress that Eq. (A10) is inapplicable to singular $\mathbf{J}_\mathrm{s}^{(0)}(\mathbf{n})$, e.g., given by Eq. (99), since such source distribution is not square integrable. Formally trying to approximate the delta function with smooth ones leads to unbounded W_0, which is consistent with the $r_\mathrm{s}\to\infty$ limit of Eq. (100).

The above result can be generalized to any $\mathbf{J}_\mathrm{s}^{(0)}(\mathbf{n})$ that is smooth inside an open region on a unit sphere and equal to zero otherwise (thus, nonsmooth on the boundary). This may correspond to the aperture of a lens that produces a beam, and leads to an additional boundary in coordinates of $\mathbf{n}'$, changing the upper limit of integration over v in Eq. (A8) and introducing v-dependent

integration limits in Eq. (A9). Both of the latter would depend on $\mathbf{n}$, since we aligned the axes of $\mathbf{n}'$ with it. It is expected that the following will only change the oscillating term in Eq. (A10), still keeping it bounded.

[1] D. S. Saxon, *Lectures on the Scattering of Light*, Scientific Report No. 9 (Department of Meteorology, University of California at Los Angeles, Los Angeles, CA, 1955).

[2] C. Müller, *Foundations of the Mathematical Theory of Electromagnetic Waves* (Springer, Berlin, 1969).

[3] M. I. Mishchenko, *Electromagnetic Scattering by Particles and Particle Groups: An Introduction* (Cambridge University, Cambridge, England, 2014).

[4] J. G. Van Bladel, *Electromagnetic Fields*, 2nd ed. (Wiley, New York, 2007).

[5] M. A. Yurkin and M. I. Mishchenko, Phys. Rev. A **97**, 043824 (2018).

[6] M. I. Mishchenko and M. A. Yurkin, J. Quant. Spectrosc. Radiat. Transfer **214**, 158 (2018).

[7] M. A. Yurkin and M. I. Mishchenko, J. Quant. Spectrosc. Radiat. Transfer **219**, 105 (2018).

[8] C. F. Bohren and D. R. Huffman, *Absorption and Scattering of Light by Small Particles* (Wiley, New York, 1983).

[9] R. Carminati, A. Cazé, D. Cao, F. Peragut, V. Krachmalnicoff, R. Pierrat, and Y. De Wilde, Surf. Sci. Rep. **70**, 1 (2015).

[10] E. Purcell, Phys. Rev. **69**, 681 (1946).

[11] L. Novotny and B. Hecht, *Principles of Nano-Optics*, 2nd ed. (Cambridge University, Cambridge, England, 2012).

[12] E. L. Ru and P. Etchegoin, *Principles of Surface-Enhanced Raman Spectroscopy: And Related Plasmonic Effects* (Elsevier, New York, 2008).

[13] N. Geuquet and L. Henrard, Ultramicroscopy **110**, 1075 (2010).

[14] N. W. Bigelow, A. Vaschillo, V. Iberi, J. P. Camden, and D. J. Masiello, ACS Nano **6**, 7497 (2012).

[15] G. D. Bernasconi, J. Butet, V. Flauraud, D. Alexander, J. Brugger, and O. J. F. Martin, ACS Photonics **4**, 156 (2017).

[16] M. Paulus and O. J. F. Martin, J. Opt. Soc. Am. A **18**, 854 (2001).

[17] M. A. Yurkin and A. G. Hoekstra, J. Quant. Spectrosc. Radiat. Transfer **106**, 558 (2007).

[18] M. A. Yurkin and A. G. Hoekstra, User manual for the discrete dipole approximation code ADDA 1.3b4 (2014), https://github.com/adda-team/adda/raw/v1.3b4/doc/manual.pdf

[19] S. D'Agostino, F. Della Sala, and L. C. Andreani, Phys. Rev. B **87**, 205413 (2013).

[20] M. A. Mahmoud, Langmuir **29**, 6253 (2013).

[21] F. Todisco, S. D'Agostino, M. Esposito, A. I. Fernàndez-Domìnguez, M. De Giorgi, D. Ballarini, L. Dominci, I. Tarantini, M. Cuscunà, F. Della Sala, G. Gigli, and D. Sanvitto, ACS Nano **9**, 9691 (2015).

[22] H. Greiner and O. J. F. Martin, Proc. SPIE **5214**, 248 (2004).

[23] E. Zubko, K. Muinonen, Y. Shkuratov, G. Videen, and T. Nousiainen, J. Quant. Spectrosc. Radiat. Transfer **106**, 604 (2007).

[24] A. D. Yaghjian, IEEE Proc. **68**, 248 (1980).

[25] M. A. Yurkin and A. G. Hoekstra, J. Quant. Spectrosc. Radiat. Transfer **112**, 2234 (2011).

[26] D. A. Smunev, P. C. Chaumet, and M. A. Yurkin, J. Quant. Spectrosc. Radiat. Transfer **156**, 67 (2015).

[27] D. S. Jones, Lond. Edinb. Dubl. Phil. Mag. **46**, 957 (1955).

[28] H. C. van de Hulst, *Light Scattering by Small Particles* (Dover, New York, 1981).

[29] C.-A. Guérin, B. Gralak, and A. Tip, Phys. Rev. E **75**, 056601 (2007).

[30] G. W. Hanson and A. B. Yakovlev, *Operator Theory for Electromagnetics: An Introduction* (Springer, New York, 2002).

[31] L. Zhu, Y. Guo, and S. Fan, Phys. Rev. B **97**, 094302 (2018).

[32] E. A. Marengo, IEEE Trans. Antennas Propag. **61**, 2164 (2013).

[33] J. D. Jackson, *Classical Electrodynamics*, 3rd ed. (Wiley, New York, 1998).

[34] V. Markel and E. Poliakov, Phil. Mag. B **76**, 895 (1997).

[35] D. R. Lytle II, P. S. Carney, J. C. Schotland, and E. Wolf, Phys. Rev. E **71**, 056610 (2005).

[36] A. G. Polimeridis, M. T. H. Reid, S. G. Johnson, J. K. White, and A. W. Rodriguez, IEEE Trans. Antennas Propag. **63**, 611 (2015).

[37] M. I. Mishchenko and M. A. Yurkin, Opt. Lett. **44**, 419 (2019).

[38] L. Novotny, Appl. Phys. Lett. **69**, 3806 (1996).

[39] S. M. Hein and H. Giessen, Phys. Rev. Lett. **111**, 026803 (2013).

[40] S. D'Agostino, F. Della Sala, and L. C. Andreani, Photon. Nanostruct. Fundam. Applic. **11**, 335 (2013).

[41] C. Vandenbem, D. Brayer, L. S. Froufe-Pérez, and R. Carminati, Phys. Rev. B **81**, 085444 (2010).

[42] Z. Zhao, Y. Shi, K. Chen, and S. Fan, Phys. Rev. A **98**, 013845 (2018).

[43] P. Anger, P. Bharadwaj, and L. Novotny, Phys. Rev. Lett. **96**, 113002 (2006).

[44] M. A. Yurkin, V. P. Maltsev, and A. G. Hoekstra, J. Opt. Soc. Am. A **23**, 2578 (2006).

[45] B. T. Draine, Astrophys. J. **333**, 848 (1988).

[46] K. Schmidt, M. A. Yurkin, and M. Kahnert, Opt. Express **20**, 23253 (2012).

[47] C. J. R. Sheppard, J. Opt. Soc. Am. A **18**, 1579 (2001).

[48] D. McGloin and K. Dholakia, Contemp. Phys. **46**, 15 (2005).

[49] G. A. Siviloglou, J. Broky, A. Dogariu, and D. N. Christodoulides, Phys. Rev. Lett. **99**, 213901 (2007).

[50] M. A. Yurkin and M. Huntemann, J. Phys. Chem. C **119**, 29088 (2015).

[51] D. L. Lager and R. J. Lytle, *Fortran Subroutines for the Numerical Evaluation of Sommerfeld Integrals Unter Anderem* (Lawrence Livermore Laboratory, Livermore, CA, 1975).

[52] G. Y. Panasyuk, J. C. Schotland, and V. A. Markel, J. Phys. A **42**, 275203 (2009).

[53] A. Small, J. Fung, and V. N. Manoharan, J. Opt. Soc. Am. A **30**, 2519 (2013).

[54] S. Zeng, D. Baillargeat, H.-P. Ho, and K.-T. Yong, Chem. Soc. Rev. **43**, 3426 (2014).

[55] D. Torrungrueng, B. Ungan, and J. T. Johnson, IEEE Geosci. Remote Sens. Lett. **1**, 131 (2004).